NASA CR-
144535

TEXAS A&M UNIVERSITY

THE DESIGN, ANALYSIS AND EXPERIMENTAL EVALUATION OF AN ELASTIC MODEL WING

by

Ralph K. Cavin, III and Chavalit Thisayakorn

DEPARTMENT OF ELECTRICAL ENGINEERING
College Station, Texas

(NASA-CR-144535) THE DESIGN, ANALYSIS AND EXPERIMENTAL EVALUATION OF AN ELASTIC MODEL WING (Texas A&M Univ.) 51 p HC $4.25 N76-10092
CSCL 01C Unclas
G3/05 39397

THE DESIGN, ANALYSIS AND EXPERIMENTAL EVALUATION OF AN ELASTIC MODEL WING

by

Ralph K. Cavin, III and Chavalit Thisayakorn

NAS 9-11303

September 1974
Department of Electrical Engineering
Texas A&M University

TABLE OF CONTENTS

LIST OF TABLES

LIST OF FIGURES

THE DESIGN, ANALYSIS, AND EXPERIMENTAL
EVALUATION OF AN ELASTIC MODEL WING

by

Ralph K. Cavin, III, and Chavalit Thisayakorn

(I) Introduction

It is common practice in preliminary static aeroelastic analyses to estimate elastic increments in stability derivatives by utilizing a clamped-vehicle stiffness matrix in conjunction with an aerodynamic influence matrix determined for the configuration by use of the linear, inviscid aerodynamic theory. These aeroelastic estimates are normally refined by 'freeing' the structure and including vehicle mass effects based upon the use of mean axis vehicle coordinate systems. [1] The computer program FLEXSTAB, which was written by The Boeing Airplane Company under the sponsorship of NASA-AMES, is a relatively sophisticated implementation of these basic ideas. FLEXSTAB has the capability of admitting two different types of structural representations. If the structural characteristics of the vehicle are adequately represented by the interconnection of beam elements, then FLEXSTAB accepts the beam EI and GK characteristics and generates the required structural matrices. On the other hand, the structural matrices can be generated externally in a finite element program, without the restriction of beam-like structural properties, and the results can be entered directly into FLEXSTAB.

The primary objective of this study was to develop experimental data from a carefully controlled elastic model to be used in evaluating the effectiveness of aeroelasticity programs such as FLEXSTAB for vehicles of the orbiter class. In order to accomplish this objective at a minimum cost it was decided to utilize an existing rigid 5% fuselage model for the 002 Orbiter configuration, and to construct elastic wings for the model. The 002 Orbiter wings were straight with moderate aspect ratio and were therefore amenable to a beam-like structural representation.

(II) Design and Fabrication of the Elastic Wing

In view of the assumed beam-like structure of the 002 Orbiter wing, it was decided that the load carrying member of the model wing should be a beam with well defined EI and GK characteristics. It was further decided that the distribution of EI and GK along the wing span should parallel the 002 EI and GK shapes provided to A&M by the NASA-JSC Structures group. However, no attempt was made to scale the given (Stiff) beam characteristics to the 5% model. Rather the selection of EI and GK was based upon the criterion that measurable deformations and stability derivative changes should occur under expected aerodynamic load.

The basic design philosophy that evolved was that the aerodynamic loads should be transmitted to the beam via rib members. Further, in order to approximate the finite-element aerodynamic methods, the wing surface was segmented in a streamwise manner and each segment was rigidly attached to a corresponding rib element. Figure 1 is a planform view showing location of the Elastic Axis, as well as the basic aerodynamic sections for the wing. The NACA airfoil descriptions are given in Figure 2. As can be seen from Figure 1, the elastic axis is swept aft at an angle of 9.75 degrees from the vertical.

Figure 3 depicts the basic construction of the elastic wing. Note that each panel section is made of low density Balsa Wood which is cemented to the supporting rib member. The region between adjacent panel sections is approximately 1/16" wide and is filled with an ultra soft Neoprene gasket that

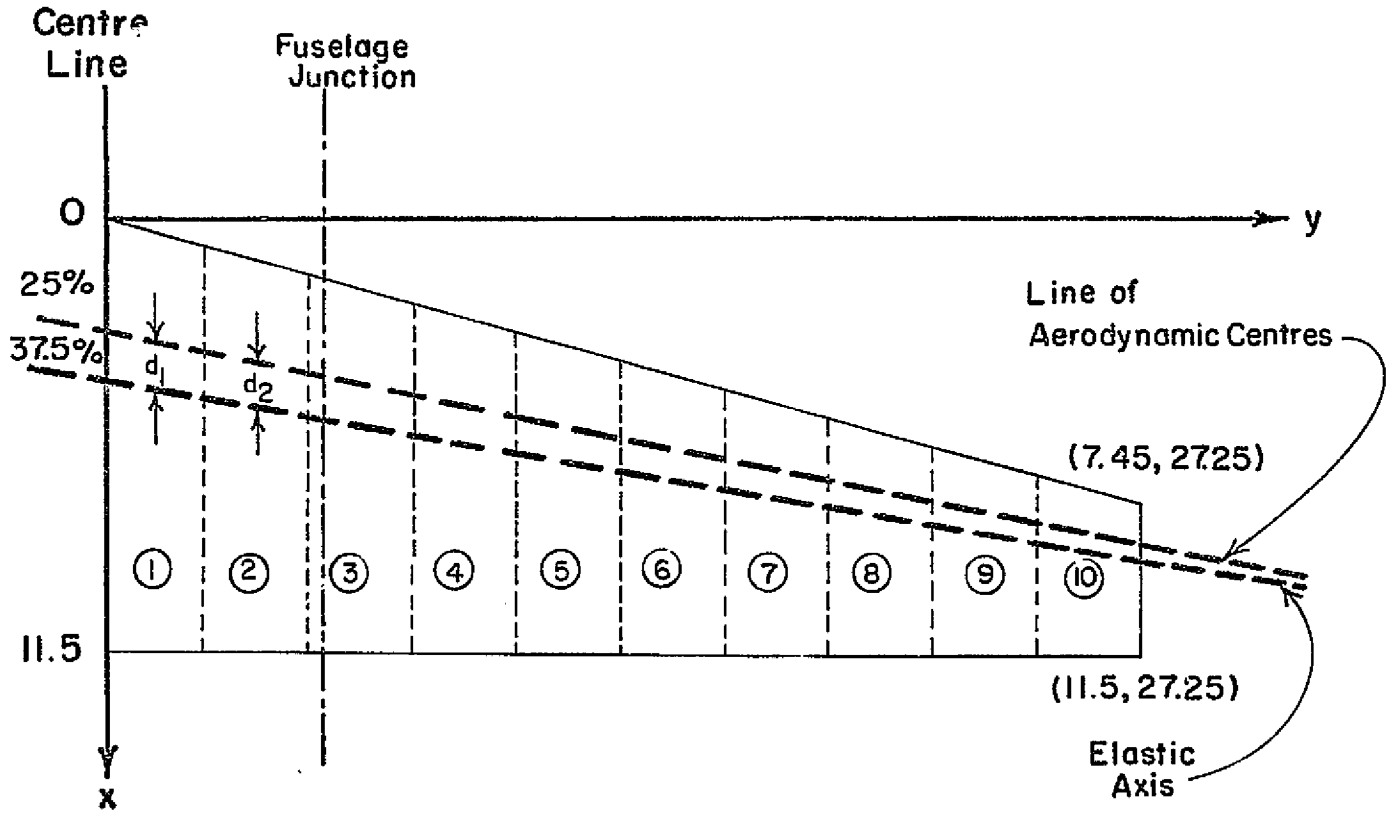

FIGURE 1. Elastic Model Wing Planform (5% 002 orbiter wing)

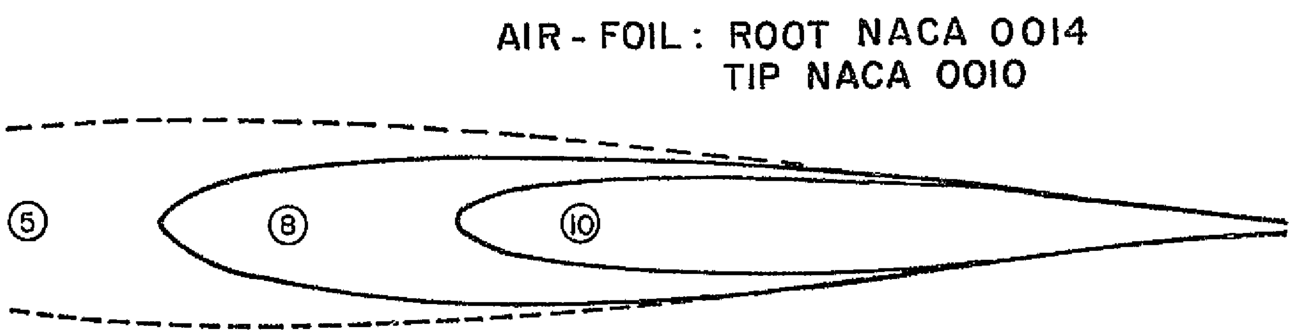

FIGURE 2. Rib-Airfoil (full size model wing cross-sections)

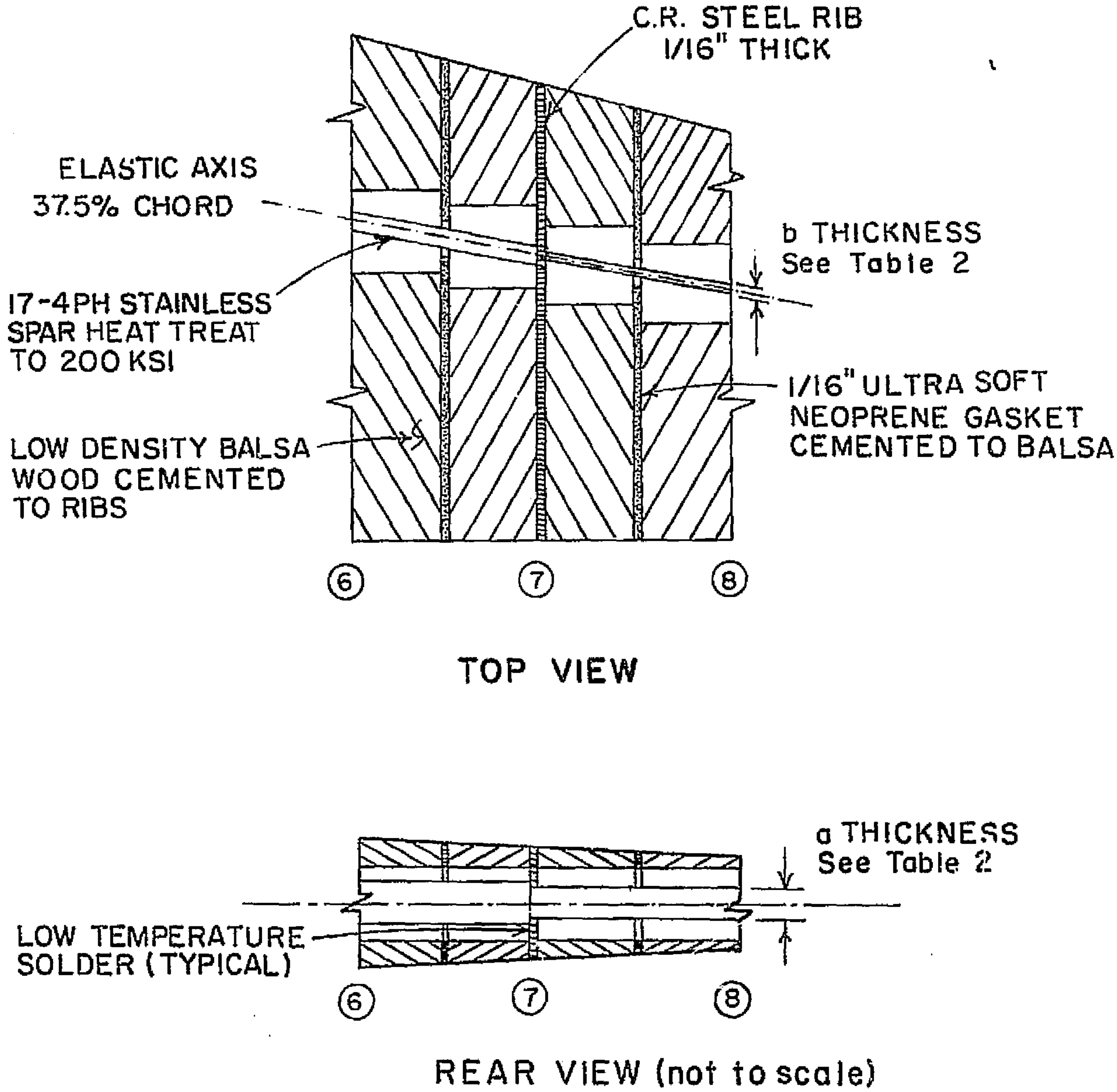

FIGURE 3. Cross-Sectional structural description at the Model-Wing Construction.

is cemented to the Balsa. Stress Calculations indicated that a high strength alloy of stainless steel could be used for the wing spar but that heat treatment was required after machining. This process allowed a 2.5 safety factor on ultimate strength and about 2.3 on yield strength. (No allowance was made for dynamic loads.) Ribs were made of the same material as the spar for ease of attachment. The spar was designed to have a rectangular cross section so that the rib elements could be firmly attached to the spar. Table 1 contains the dimensional data for the spar. The computed values for EI and GK are also listed in this table. The cross sectional moment data which was computed by using the formulae [4]

$$K = \frac{ba^3}{3} - \frac{64a^4}{\pi^5}\tanh\left(\frac{\pi b}{2a}\right) . \qquad (1)$$

$$I_x = \int z^2 \, dA = \frac{ba^3}{12} \qquad (2)$$

The above symbols are defined in Figure 4.

(III) Design Calculations

The purpose of this section is to describe the analysis methods that were utilized in the design of the elastic wing described in Section II. Two basic analytical tools were utilized in the evolution of structural specifications for the wing; namely the Doublet Lattice Aerodynamic lifting surface procedure and the finite element structural analysis method for beam members. In the following, we first discuss the analytical formulation for the general, time-dependent problem. After this broad notational framework has been established, the special static-aeroelastic and flutter problems are considered.

A. The Structural Model

As has already been pointed out, the principal load-carrying member in the wing structure is the spar element. The spar is essentially a beam element with

Spanwise Panel (location number)	b - Thickness (inches)	a - Thickness (inches)	Lengths (inches)
2-3	0.391	0.407	1.078
3-4	0.369	0.355	2.828
4-5	0.273	0.368	2.828
5-6	0.243	0.310	2.828
6-7	0.173	0.300	2.828
7-8	0.152	0.246	2.828
8-9	0.146	0.188	2.828
9-10	0.129	0.152	2.891

Table 1. Spar Dimensions (See also Figure 3)

Station Number of Spanwise Segments	Values of EI ($lb - in^2$)	Values of GK ($lb - in^2$)
3	63687.50	40090.40
4	39837.50	27166.72
5	32875.00	15314.09
6	17575.00	8730.85
7	11325.00	3718.85
8	5468.75	1990.35
9	2343.75	1156.62
10	1093.75	600.77

Table 1. (continued)

Values of EI and GK for wing spar

$E = 2.9 \times 10^7 \quad lb/in^2$

$G = 1.12 \times 10^7 \quad lb/in^2$

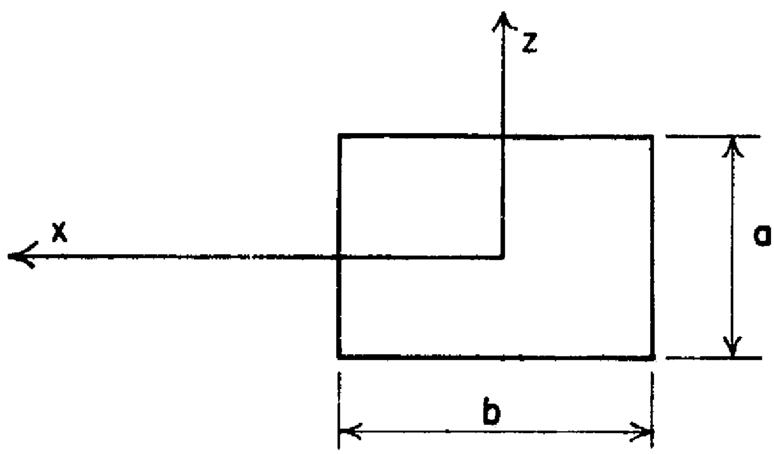

FIGURE 4. Definition of symbols for beam Cross-section.

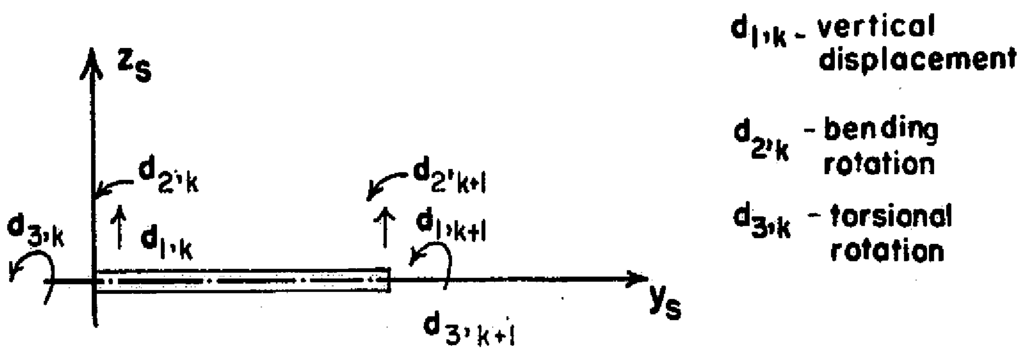

FIGURE 5. Definition of structural nodal displacements.

rectangular sections of length 2.8 in. whose sectional area progressively decreases in the spanwise direction. There are 8 spar sections, each with a possibility of 6 physical degrees of freedom per section, implying a maximum of 48 structural degrees of freedom. However, in view of the planned testing of the wing at very small (less than ten degrees) angles of attack, it was decided that in-plane bending of the spar would be minimal and hence only torsional and normal bending degrees of freedom were retained for each beam element. The degrees of freedom associated with each element are defined in Figure 5. The elemental stiffness matrix for the member shown in Figure 5 therefore reduces to [2].

$$
[K]_x = \begin{array}{c}
\begin{array}{cccccc} d_{1,K} & d_{2,K} & d_{3,K} & d_{1,K+1} & d_{2,K+1} & d_{3,K+1} \end{array} \\
\left[\begin{array}{cccccc}
12\, EI_x/\ell^3, & & & & & \\
6\, EI_x/\ell^2, & 4\, EI_x/\ell\ , & & & \text{symmetric} & \\
0 \ , & 0 \ , & GK/\ell, & & & \\
-12\, EI_x/\ell^3, & -6\, EI_x/\ell^2, & 0 \ , & 12\, EI_x/\ell^3, & & \\
-6\, EI_x/\ell^2, & 0 \ , & 0 \ , & -6\, EI_x/\ell^2, & 4\, EI_x/\ell, & \\
0 \ , & 0 \ , & GK/\ell, & 0 \ , & 0 \ , & GK/\ell
\end{array}\right]
\end{array}
\tag{3}
$$

A composite stiffness matrix can be generated by appropriately combining the element matrices in an underlying structural reference frame. In view of the fact that the spar is straight, the assembly task is quite straight-forward in this case and can be accomplished by overlaying successive element matrices and adding overlapping terms, e.g.,

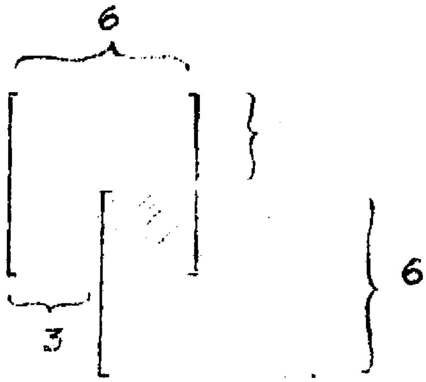

Of course the left end of the inboard spar element is constrained to have no degrees of freedom since the flexible wing is attached to the fuselage at this point.

A generalized mass matrix can be formulated for the flexible wing by using the results given in [2], i.e., the mass matrix for the element in Figure 5 is

$$
\begin{array}{cc}
 & \begin{array}{cccccc} d_{1,K} & d_{2,K} & d_{3,K} & d_{1,K+1} & d_{2,K+1} & d_{3,K+1} \end{array} \\
[M]_K = & \left[\begin{array}{cccccc}
\frac{13}{35} + \frac{6I_x}{5A\ell^2} & & & & & \\
\frac{11\ell}{210} + \frac{I_x}{10A\ell} & \frac{\ell^2}{105} \quad \frac{2I_x}{15A} & & \text{symmetric} & & \\
0 & 0 & \frac{J_y}{3A} & & & \\
\frac{9}{70} - \frac{6I_x}{5A\ell^2} & \frac{13\ell}{420} - \frac{I_x}{10AC} & 0 & \frac{13}{35} + \frac{6I_x}{5AC^2} & & \\
-\frac{13\ell}{420} + \frac{I_x}{10A\ell} & \frac{-\ell^2}{140} - \frac{I_x}{30A} & 0 & \frac{-11\ell}{210} - \frac{I_x}{10A\ell} & \frac{\ell^2}{105} + \frac{2I_x}{15A} & \\
0 & 0 & \frac{J_y}{6A} & 0 & 0 & \frac{J_y}{3A}
\end{array}\right]
\end{array}
\qquad (4)
$$

As in the case of the stiffness matrix, assembly of a composite mass matrix for the wing can be accomplished by appropriately combining the matrices, $[M]_K$, $K = 1,..,8$. The effects of rib mass were included by simply adding lumped mass and inertia terms to the diagonal elements of the spar mass matrix. A summary of rib mass properties is given in Table 2.

Station number of ribs	Distances of ribs' c.g. off from the elastic axis (in.)	Rib mass (slug) x 10^{-3}	Polar Mass moment of inertia (slug-in^2) x 10^{-2}
3	0.706527	0.243999	0.140291
4	0.651691	0.201206	0.098401
5	0.596856	0.163412	0.067019
6	0.542019	0.130345	0.044076
7	0.487183	0.101735	0.027786
8	0.432345	0.077311	0.016626
9	0.377509	0.0568	0.009311
10	0.322672	0.039931	0.004781

Table 2. Data on steel ribs of the wing

Since the wing spar is swept at an angle, Λ, of 9.75 degrees, it is necessary to transform the spar structural matrices into a coordinate frame compatible with the aerodynamic frame. This is easily accomplished by performing the following transformation

$$[K]_1 = [T]\,[K]\,[T]^T$$

$$\text{where} \qquad T = \begin{bmatrix} 1 & 0 & 0 & 0 & 0 & 0 \\ 0 & \cos\Theta & -\sin\Theta & 0 & 0 & 0 \\ 0 & \sin\Theta & \cos\Theta & 0 & 0 & 0 \\ 0 & 0 & 0 & 1 & 0 & 0 \\ 0 & 0 & 0 & 0 & \cos\Theta & -\sin\Theta \\ 0 & 0 & 0 & 0 & \sin\Theta & \cos\Theta \end{bmatrix}$$

B. Aerodynamics Development

The basic procedure that has been used to treat aerodynamic forces is based on the Doublet-Lattice-Method (D.L.M.) [3]. Fundamentally, the D.L.M. yields a set of Aerodynamic Influence Coefficients, [D], relating the assumed harmonic motion of the normal wash, {w}, at specified points on the wing surface to the pressure differential, {ΔCp}, across the wing. Specifically, the integral equation

$$w(x,y,z) = \frac{1}{8\pi} \iint_{\text{lifting surface}} K(x-\xi,\ y-\eta,\ z-\zeta;\ \omega, M)\,\Delta Cp\, d\xi\, d\sigma \tag{5}$$

is approximately solved as

$$\{w\} = [D]\,\{\Delta Cp\} \tag{6}$$

where the velocity normal to the oscillating surface is

$$\{W\} = U_\infty \operatorname{Re}\left[\{w\}\, e^{i\omega t}\right], \tag{7}$$

and the pressure differential is

$$\{\Delta p\} = q_\infty \operatorname{Re}\left[\{\Delta Cp\}\, e^{i\omega t}\right]. \tag{8}$$

Let us now consider specifically the computation of the aerodynamic forces for later use.

In general, ℓ_{ij} is the distance from the jth. structural node to the 1/4 chord point for the ij<u>th</u>. panel and r_{ij} is the distance from the j<u>th</u>. structural node to the 3/4 chord point for the ij<u>th</u>. panel (See Figure 6). The total force acting on the ij<u>th</u>. panel is given by

$$f_{ij} = \Delta p_{ij} \; A_{ij} \tag{9}$$

and will be assumed to be acting at the center of the 3/4 chord point of the ij<u>th</u>. panel. In order to define the sense of the various forces and moments due to the aerodynamic forces, we must first define the assumed positive displacement at node j. This is done in Figure 7, the force tending to increase the d_1 coordinate is

$$f_{ij} = \sum_{i=1}^{P} \Delta p_{ij} \; A_{ij}, \tag{10}$$

the force tending to increase d_2 is zero and the force tending to increase d_3 is

$$f_{3j} = -\sum_{i=1}^{P} \ell_{ij} \; \Delta p_{ij} \; A_{ij}, \text{ (a moment)} \tag{11}$$

where we assume that ℓ_{ij} and r_{ij} carry the sign of their x-coordinate location. We will further assume that there are Q spanwise panel rows and P chordwise panel rows, implying that n, the dimension of $\{d\}$ is 3Q.

Let us now consider the computation of the normal wash W in terms of the displacements at the structural node points. By definition, the normal wash must be equal to the substantial derivative of the vertical displacement of the surface. (Implying no fluid flow through the surface.) In particular, we are interested in satisfying this boundary condition at the 3/4 chord points for each panel. The vertical displacement at any point along the chordwise centerline through node j is

$$z_j = d_{1j} - xd_{3j}, \tag{12}$$

where the definitions of Figure 7 have been used. The substantial derivative is therefore

$$W_j(t) = \frac{D}{Dt}(z_j) = \dot{d}_{ij} - xd_{3j} - U_\infty d_{3j}. \tag{13}$$

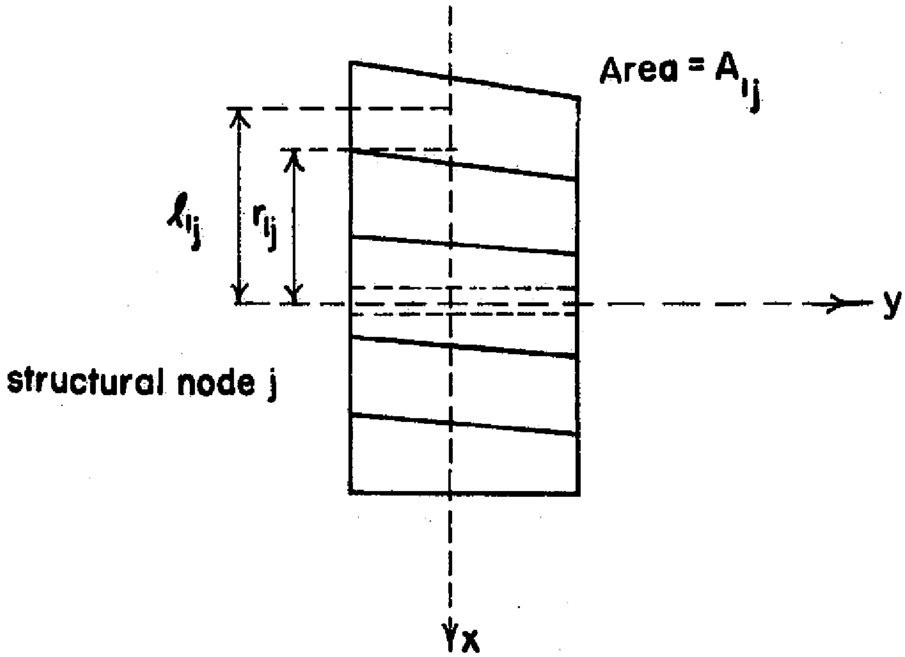

FIGURE 6. Span-wise slice of wing showing definition of symbols.

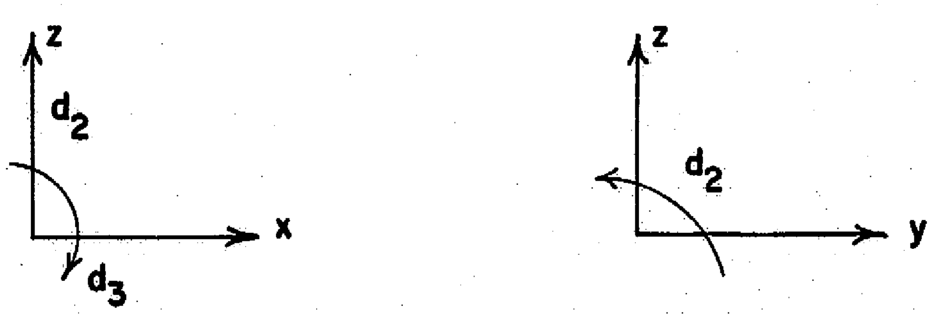

FIGURE 7. Definition of positive sense for displacements at node j.

Consequently, the downwash at the 3/4 chord of the ij<u>th</u>. panel can be written. (Assuming no chordwise deformation).

$$W_{ij}(t) = \overset{\circ}{d}_{ij} - r_{ij}\,\overset{\circ}{d}_{3j} - U_{\infty} d_{3j}. \qquad (14)$$

Further, if W_{ij} is assumed to be of exponential form,

$$W_{ij}(t) = W_{ij}\, e^{i\omega t},$$

(14) becomes

$$W_{ij} = d_{ij}(i\omega) - r_{ij}\, d_{3j}(i\omega) - U_{\infty} d_{3j} \qquad (15)$$

Let us now return to (6) and establish the mechanism for computing the generalized nodal forces. Denote

$$\{w\} = \{w_{11}\; w_{12}\; \ldots\; w_{1Q} \;|\; w_{21}\; w_{22}\; \ldots\; w_{2Q} \;|\; \ldots\ldots \;|\; w_{P1}\; w_{P2}\; \ldots\; w_{PQ}\}^T \qquad (16)$$

In (6), [D] is therefore a matrix of dimension PQ x PX. Let the force vector {f}, the pressure vector, {Δp}, etc. be defined using the same ordering as (16). In addition, let the generalized forces at node k be ordered as

f_{1k} = vertical deformation force

f_{2k} = bending deformation moment

f_{3k} = torsional deformation moment,

and define

$$\{f\}_s^T = \{f_{11}\; f_{21}\; f_{31} \;|\; f_{12}\; f_{22}\; f_{32} \;|\; \ldots\ldots \;|\; f_{1Q}\; f_{2Q}\; f_{3Q}\}, \qquad (17)$$

i.e., $\{f\}_s$ denotes the vector of forces acting at the structural nodes. We must now develop appropriate transformation matrices so that $\{f\}_s$ can be calculated in terms of nodal displacements {d}. From (10) and (11), we can write

$$\underset{3Q}{\{f\}_s} = \underset{3Q \times PQ}{[G]}\; \underset{PQ}{\{\Delta p\}} \qquad (18)$$

where the matrix [G] is defined as

$$[G] = \begin{bmatrix}
A_{11} & 0 \,.....\, 0 & A_{21} & 0 \,.....\, 0 & .... \; A_{P1} & 0 \,.....\, 0 \\
0 & 0 \,.....\, 0 & 0 & 0 \,.....\, 0 & .... \; 0 & 0 \,.....\, 0 \\
-\ell_{11}A_{11} & 0 \,.....\, 0 & -\ell_{21}A_{21} & 0 \,.....\, 0 & .... -\ell_{P1}A_{P1} & 0 \,.....\, 0 \\
0 & A_{12} \,...\, 0 & 0 & A_{22} \,...\, 0 & .... \; 0 & A_{P2} \,...\, 0 \\
0 & 0 \,.....\, 0 & 0 & 0 \,.....\, 0 & .... \; 0 & 0 \,.....\, 0 \\
0 & -\ell_{12}A_{12} \cdot\, 0 & 0 & -\ell_{22}A_{22} \cdot\, 0 & .... \; 0 & -\ell_{P2}A_{P2} \cdot\, 0 \\
\cdot & \cdot \;\cdot \;\cdot \;\cdot & \cdot & \cdot \;\cdot \;\cdot \;\cdot & \cdot \;\cdot \;\cdot \;\cdot & \cdot \;\cdot \;\cdot \;\cdot \\
0 & 0 \,.....\, A_{1Q} & 0 & 0 \,.....\, A_{2Q} & .... \; 0 & 0 \,.....\, A_{PQ} \\
0 & 0 \,.....\, 0 & 0 & 0 \,.....\, 0 & .... \; 0 & 0 \,.....\, 0 \\
0 & 0 \,.....-\ell_{1Q}A_{1Q} & 0 & 0 \,.....-\ell_{2Q}A_{2Q} & .... \; 0 & 0 \,.....-\ell_{PQ}A_{PQ}
\end{bmatrix} \tag{19}$$

Equation (6) implies that

$$\{\Delta p\} = q_\infty [D]^{-1} \{w\}. \tag{20}$$

However (15) allows the following relation between {w} and {d}.

$$\{W\} = \frac{1}{U_\infty} [H] \quad \{d\} + \frac{i\omega}{U_\infty} \; [E] \quad \{d\} \tag{21}$$

where [H] and [E] are defined by

$$[H] = \begin{array}{c}
\overbrace{\hphantom{0 \quad 0 \quad -U_\infty \quad 0 \quad 0 \quad 0 \,......\, 0 \quad 0 \quad 0}}^{3Q} \\
\left[\begin{array}{ccccccccc}
0 & 0 & -U_\infty & 0 & 0 & 0 \,...... & 0 & 0 & 0 \\
0 & 0 & 0 & 0 & 0 & -U_\infty ...... & 0 & 0 & 0 \\
\cdot & \cdot & \cdot & \cdot & \cdot & \cdot \;\cdot \;\cdot & \cdot & \cdot & \cdot \\
0 & 0 & 0 & 0 & 0 & 0 \,...... & 0 & 0 & -U_\infty \\
 & & & & \vdots & & & & \\
 & & & & \text{repeats P times} & & & & \\
 & & & & & & & &
\end{array}\right]
\end{array}
\begin{array}{l} \left.\vphantom{\begin{array}{c}0\\0\\ \cdot\\0\end{array}}\right\} Q \\ \\ \\ \\ \end{array}$$

$$[E] = \begin{array}{c} Q\left\{\vphantom{\begin{matrix}1\\1\\1\\1\end{matrix}}\right. \\ \vphantom{\begin{matrix}1\\1\\1\\1\\1\\1\\1\\1\end{matrix}} \end{array} \left[\begin{array}{cccccccccc}
1 & 0 & -r_{11} & 0 & 0 & 0 & \cdots & 0 & 0 & 0 \\
0 & 0 & 0 & 1 & 0 & -r_{12} & \cdots & 0 & 0 & 0 \\
\cdot & \cdot & \cdot & \cdot & \cdot & \cdot & \cdot & \cdot & \cdot & \cdot \\
0 & 0 & 0 & 0 & 0 & 0 & \cdots & 1 & 0 & -r_{1Q} \\
1 & 0 & -r_{21} & 0 & 0 & 0 & \cdots & 0 & 0 & 0 \\
0 & 0 & 0 & 1 & 0 & -r_{22} & \cdots & 0 & 0 & 0 \\
\cdot & \cdot & \cdot & \cdot & \cdot & \cdot & \cdot & \cdot & \cdot & \cdot \\
0 & 0 & 0 & 0 & 0 & 0 & \cdots & 1 & 0 & -r_{2Q} \\
\cdot & \cdot & \cdot & \cdot & \cdot & \cdot & \cdot & \cdot & \cdot & \cdot \\
1 & 0 & -r_{P1} & 0 & 0 & 0 & \cdots & 0 & 0 & 0 \\
0 & 0 & 0 & 1 & 0 & -r_{P2} & \cdots & 0 & 0 & 0 \\
\cdot & \cdot & \cdot & \cdot & \cdot & \cdot & \cdot & \cdot & \cdot & \cdot \\
0 & 0 & 0 & 0 & 0 & 0 & \cdots & 1 & 0 & -r_{PQ}
\end{array}\right] \left.\vphantom{\begin{matrix}1\\1\\1\\1\\1\\1\\1\\1\\1\\1\\1\\1\\1\end{matrix}}\right\} PQ \qquad (23)$$

If we now combine (18), (20) and (21), we can finally write

$$\{f\}_s = \frac{q_\infty}{U_\infty} [G] \; [D(\omega)]^{-1} \; \{[H] + i\omega[E]\} \; \{d\} \qquad (24)$$

C. The Static Aeroelasticity Problem

The bulk of the analytical work conducted during this study involved the estimation of elastic deformations under steady flow conditions. In this case, ω is set to zero in the aerodynamic matrices and D is defined over the field of real numbers. Hence (24) reduces to

$$\{f\}_s = \frac{q_\infty}{U_\infty} [G] \; [D]^{-1} \; [H] \; \{d\} \qquad (25)$$

Gravitational loading of the wing was neglected because it was found that these forces were small compared to expected aerodynamic forces. The result of combining (25) with the composite stiffness matrix whose development was outlined in Section III-A is the following expression

$$[K]\{d\} = \frac{q_\infty}{U_\infty}[G][D]^{-1}[H](\{d\} + \alpha\{1\}) \tag{26}$$

where {1} is a vector of length 3Q each of whose components is a one. In effect, the term in parentheses on the right hand side of (26) contains a term dependent upon the elastic deformation {d} and a term dependent upon the rigid angle of attack, α. Now it is a simple manner to indicate the solution to (26), e.g.

$$\{d\} = \left([K] - \frac{q_\infty}{U_\infty}[G][D]^{-1}[H]\right)^{-1} \frac{q_\infty}{U_\infty}[G][D]^{-1}[H]\{1\}\alpha \tag{27}$$

A computer program was written to implement (27) using the planar doublet lattice procedure (vortex lattice for steady flow) to calculate the deformed wing shape under a specified Mach number, q_∞ and rigid angle of attack, α. All theoretical aeroelasticity results described in Section IV of this report, were obtained via this procedure. A listing for this computer program is given in Appendix A.

D. Flutter Problem

The basic problem in flutter analysis is that of determining if the wing will develop oscillatory motions under test conditions. This requires the inclusion of appropriate mass matrices and an unsteady aerodynamics capability into the existing computer code).

By utilization of matrix structural analysis methods, discrete mass and stiffness matrices have been developed for the wing under consideration (See Section III). The resulting differential equation assumes the classical form

$$[M]\{\ddot{d}(t)\} + [K]\{d(t)\} = \{F_A(t)\}, \tag{28}$$

where $[M]$ = mass matrix

$[K]$ = stiffness matrix

$\{d(t)\}$ = displacement vector for the structure

$\{F_A(t)\}$ = the applied aerodynamic forces.

The basic approach was to ascertain those frequencies at which harmonic motion can exist as a solution to (28).

It is normally convenient in structural analysis applications to work with the frequencies and mode shapes associated with the unexcited structural system. If we set $\{F_A(t)\}$ to zero in (28) and assume

$$\{d(t)\} = \{d\}\, e^{i\omega t}, \tag{29}$$

then (28) becomes, upon rearranging:

$$(\omega^2 I - [M]^{-1} [K])\, \{d\} = \Theta \tag{30}$$

It is clear therefore that the natural frequencies for the free system correspond to the eigenvalue of $[M]^{-1}$ $[K]$ and mode shapes $\{d\}$ correspond to the eigenvectors of $[M]^{-1}$ $[K]$. Let us denote the eigenvalues by ω_i and the associated eigenvectors by $\{p_i\}$, where $i = 1, 2, \ldots , n$. (n is the dimension of $\{d\}$.) Define

$$[P] = [\{p_1\}\ \{p_2\}\ \ldots .\ \{p_n\}] \tag{31}$$

$$[\Omega] = \text{diagonal}\ [\omega_1^2\ \omega_2^2\ \ldots .\ \omega_n^2]. \tag{32}$$

The natural frequencies in radians per second are tabulated below:

5.241×10^{10}	1.305×10^{9}
3.121×10^{10}	7.982×10^{8}
1.970×10^{10}	5.578×10^{8}
1.320×10^{10}	4.788×10^{8}
1.177×10^{10}	2.383×10^{8}
7.810×10^{9}	1.121×10^{8}
7.123×10^{9}	5.220×10^{7}
4.483×10^{9}	3.524×10^{7}
4.065×10^{9}	1.992×10^{7}
3.258×10^{9}	5.589×10^{6}
2.151×10^{9}	1.059×10^{6}
1.789×10^{9}	9.588×10^{4}

Table - List of squared natural frequencies - $(\text{rad/sec})^2$

If we return to (28) and assume that the solution $\{d(t)\}$ is written as a linear combination of the basic vectors of $[P]$ with time varying coefficient, we have

$$\{d(t)\} = \sum_{i=1}^{n} \phi_i(t) \; \{p_i\} \tag{33}$$

The $\phi_i(t)$ are unknown scalar functions of time. We can place (33) into vector-matrix form by defining

$$\{\phi^T(t)\} = \{\phi_1(t) \cdot \phi_2(t) \; \dots . \; \phi_n(t)\} \tag{34}$$

and writing

$$\{d(t)\} = [P] \; \{\phi(t)\} \tag{35}$$

The substitution of (35) into (28), with some manipulations, yields

$$\{\overset{\circ\circ}{\phi}(t)\} + [\Omega] \; \{\phi(t)\} = [P]^{-1} \; [M]^{-1} \; \{F_A(t)\}. \tag{36}$$

It follows therefore that by the introduction of the coordinates ϕ_i, $i = 1, 2, \dots, n$, the left hand side of (36) is decoupled and hence amenable to straight forward solution. However, the right hand side of (36), which has only been written in functional form to this point, is in fact a rather involved function of $\{d(t)\}$. With the substitution of (24) into (36), the dynamical equation for the elastic wing finally becomes

$$\{-\omega^2 I + [\Omega]\} \; \{\phi(\omega)\} = \{[S(\omega)] + i\omega[T(\omega)]\} \; \{\phi(\omega)\} \tag{37}$$

where
$$[S(\omega)] = \frac{q_\infty}{U_\infty} \; [P]^{-1} \; [M]^{-1} \; [G] \; [D(\omega)]^{-1} \; [H] \; [P] \tag{38}$$

$$[T(\omega)] = \frac{q_\infty}{U_\infty} \; [P]^{-1} \; [M]^{-1} \; [G] \; [D(\omega)]^{-1} \; [E] \; [P]. \tag{39}$$

The inverse Fourier Transform of (37) is

$$\{\overset{\circ\circ}{\phi}(t)\} - [T(t)] * \{\overset{\circ}{\phi}(t)\} + [\Omega] \; \{\phi(t)\} - [S(t)] * \{\phi(t)\} = 0 \tag{40}$$

where

$$[S(t)] = \mathcal{F}^{-1} \; \{[S(\omega)]\}$$
$$[T(t)] = \mathcal{F}^{-1} \; \{[T(\omega)]\}$$

and * denotes the convolution operation. The investigation for instability or sustained oscillation modes for the elastic wing is now reduced to that of finding the location of the roots for the characteristic equation of system (40). Unfortunately, closed form expressions are not available for the elements of $[T(t)]$ and $[S(t)]$ due to the fact that $[D(\omega)]$ can only be computed numerically for specified values of ω. Tests were made to determine if any of the lower natural frequencies corresponded to eigenvalues for (40) and it was determined that they did not.

(IV) Description of Tests

Essentially two types of tests were conducted on the elastic wing after it had been fabricated at the Texas A&M Model Shop.

(A) Static Tests

The vortex lattice program was utilized to compute the aerodynamic loads that could be expected to act on each streamwise row of panels if the wing was rigid. The loads were computed for an angle of attack of 5° and $q_\infty = 80.\text{lbs/ft.}^2$ Weights equal to these spanwise loads were attached to the 1/4 chord point for each panel section. Then vertical displacement measurements were made for each rib at 25% and 75% of rib length. By using these measurements and data on the unloaded wing position it was possible to calculate the wing elastic pitching rotation.

(B) Wind Tunnel Tests

A series of six wind tunnel tests were conducted at the Texas A&M University Wind Tunnel for two orbiter configurations. The conditions were:

$$q_\infty = 50 \text{ lb/ft}^2;\ \alpha = 2^\circ,\ 5^\circ,\ \&\ 8^\circ$$
$$q_\infty = 80 \text{ lb/ft}^2;\ \alpha = 2^\circ,\ 5^\circ,\ \&\ 8^\circ$$

The elevon setting was held at zero for all tests. These tests were conducted for the Orbiter with elastic wings and they were repeated for the Orbiter with identical rigid wings. The standard force and moment data, C_L, C_D, and C_M, were recorded for each sequence of tests. In addition, a Cathatometer was utilized to make vertical displacement measurements at each spanwise rib location for both the leading and trailing edges of the wing. The Cathatometer was instrumented with a potentiometer so that displacement readings could be automatically read into the wind tunnel digital computer. One difficulty that was experienced during the conduct of the test sequence was that the Cathatometer had to be moved in order to make both leading edge and trailing edge measurements. Due to the unevenness of the floor, the reference point was therefore shifted causing some difficulty in checking test repeatability.

(V) Comparison of Analytical and Experimental Results

As indicated in Section IV, a series of static load tests were conducted to verify that the structural model used for the wing in the computer program was in good agreement with the elastic deformations actually given by the wing. Figures 8 and 9 show curves of vertical deflection and elastic twist about the y axis derived from both experimental and analytical procedures. It is clear that good correlation was obtained for both twist and displacement in the static case, implying that the mathematical characterization of the wing was adequate.

Figures 10, 11, and 12 summarize some of the deformation and force data collected during the wind tunnel program. Figure 10 reflects the expected result that increased rigid angle of attack yielded increased z - direction deformations. Further, for a given q_∞ and α, z - deflections increased uniformly in going from the wing root to the wing tip. Figure 11 provides a comparison of C_L for the elastic and rigid models obtained from experimental procedure. These curves are so close to rigid C_L obtained from the analytical procedure that the latter has been omitted from the Figure. Finally, Figure 12 displays the elastic twist (increment in angle of attack) at $\alpha = 8$ degrees for $q_\infty =$ 50 lb/ft^2 and 80 lb/ft^2. It is interesting to observe that a small negative

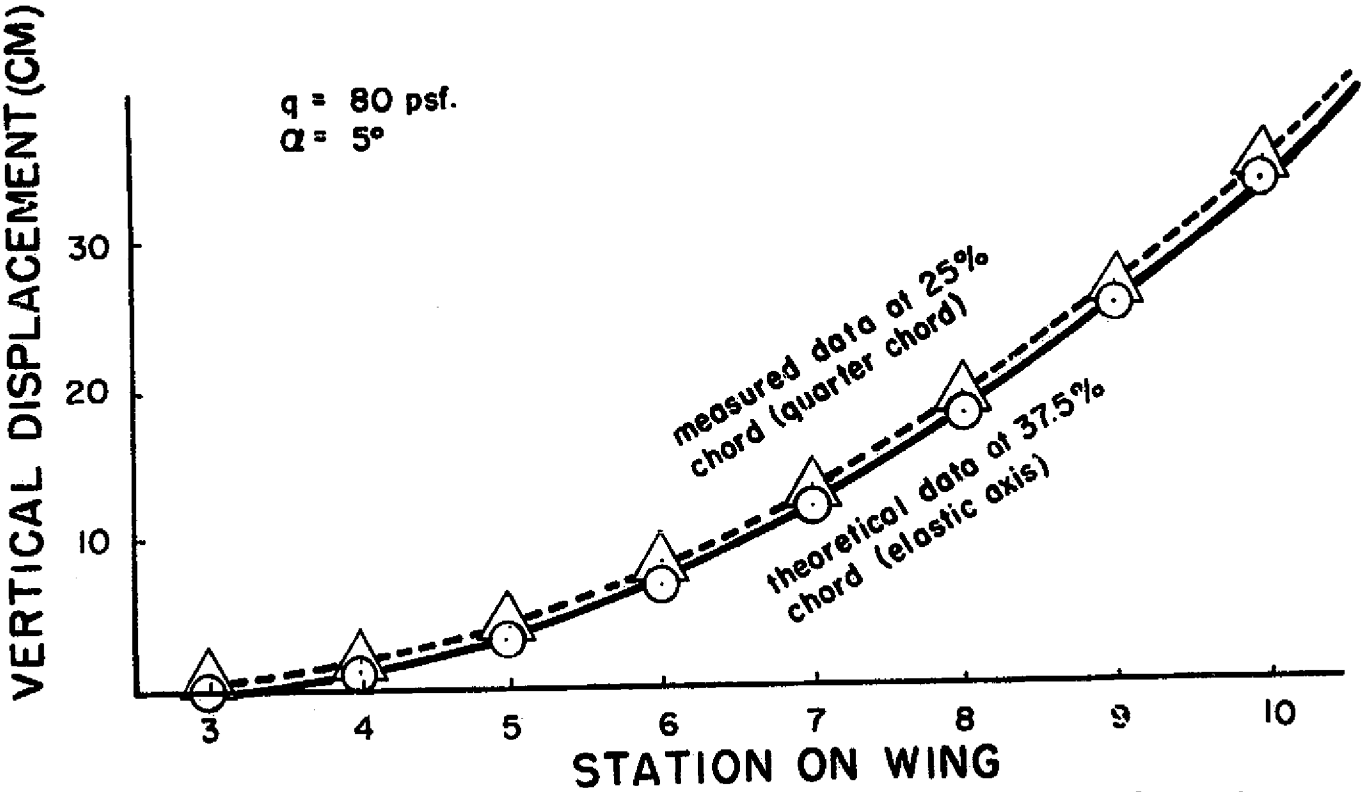

FIGURE 8. Comparison of the static load test linear deflections. Note that the deflection along the leading edge is in general larger than along the trailing edge.

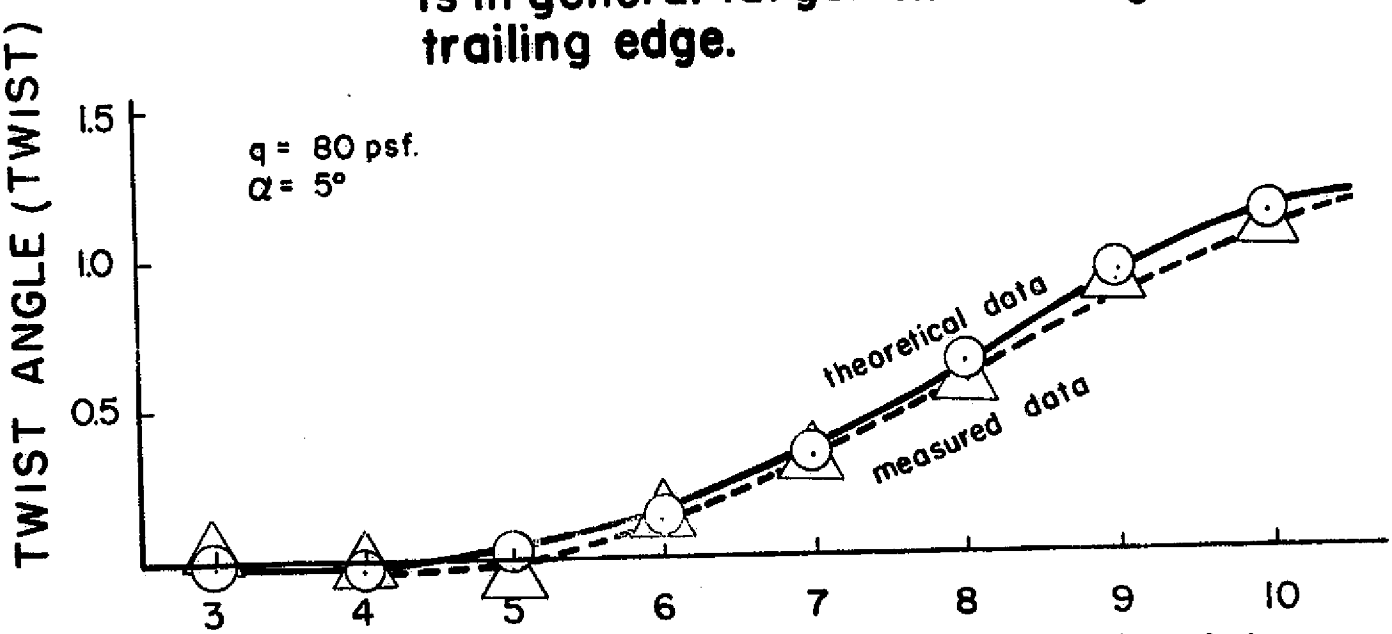

FIGURE 9. Comparison of the static load twist angle.

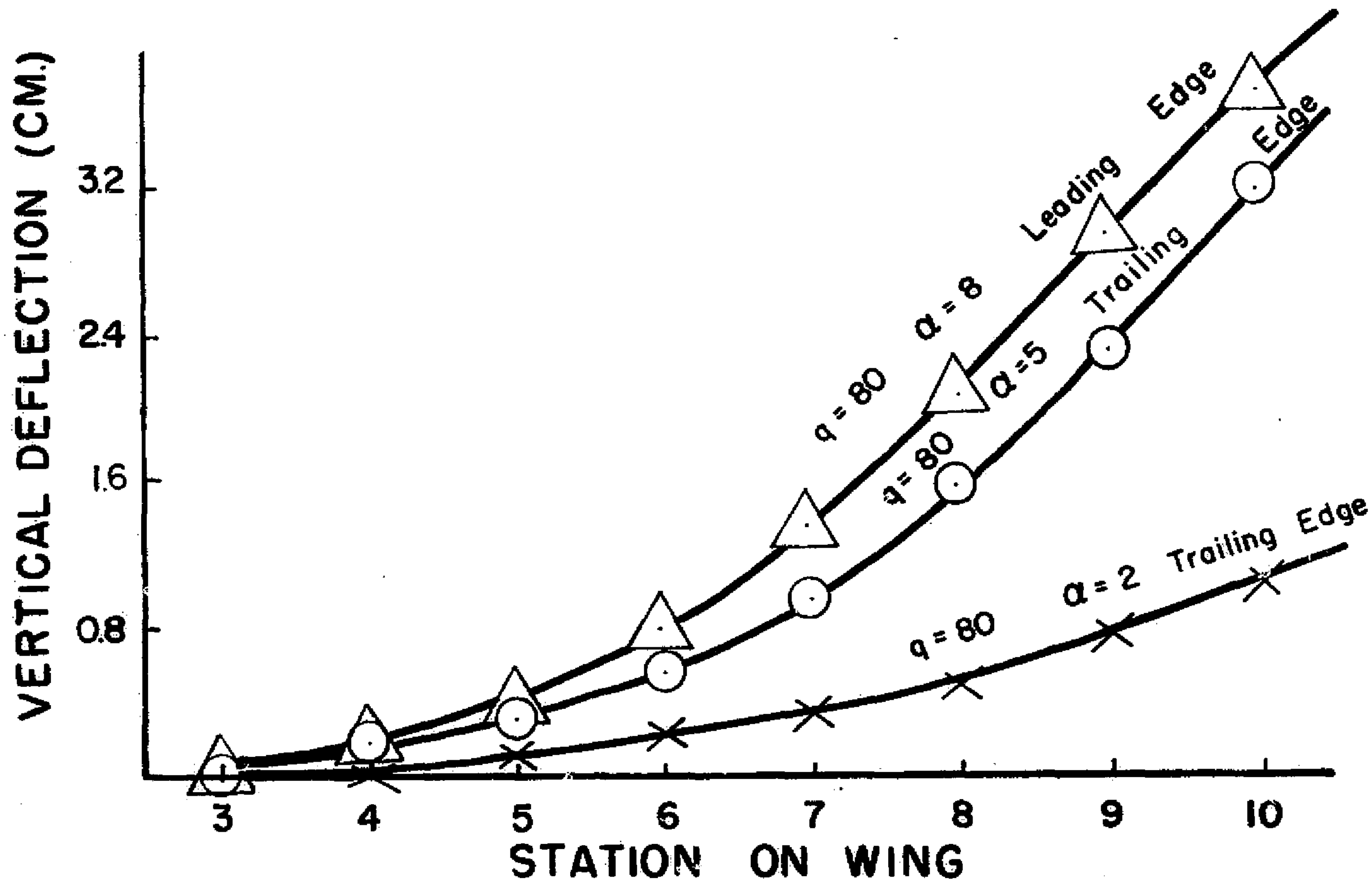

FIGURE 10. Plots of vertical deflections (in centimeters) measured in the wind tunnel.

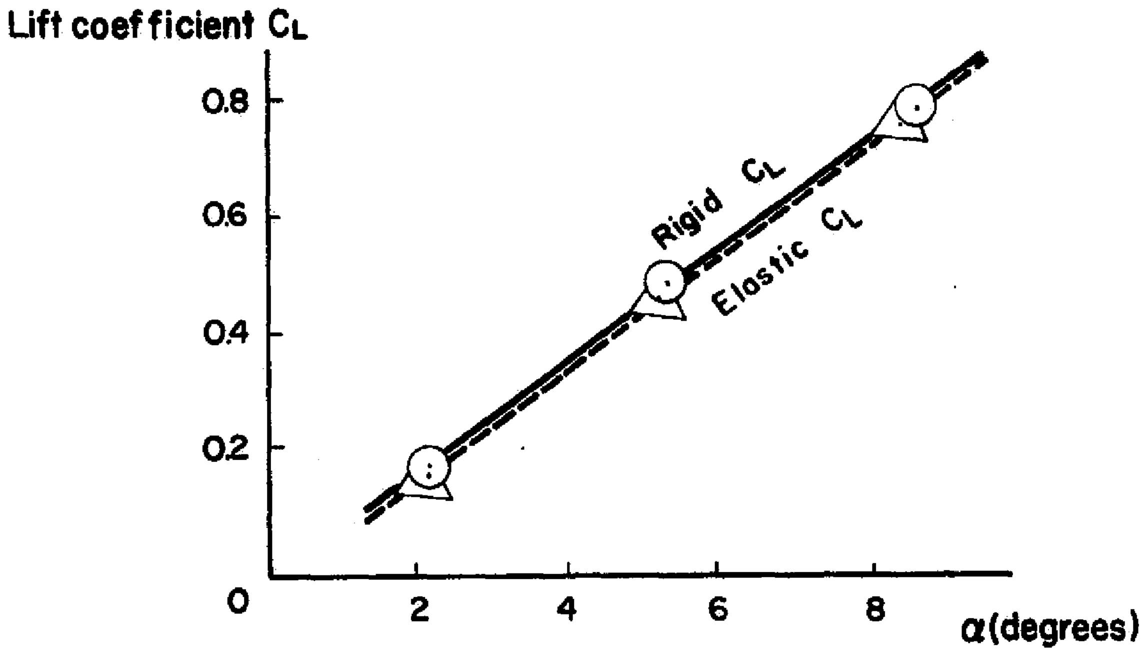

FIGURE II-a. Lift coefficient C_L versus angle of attack α, q=50 (leading edge).

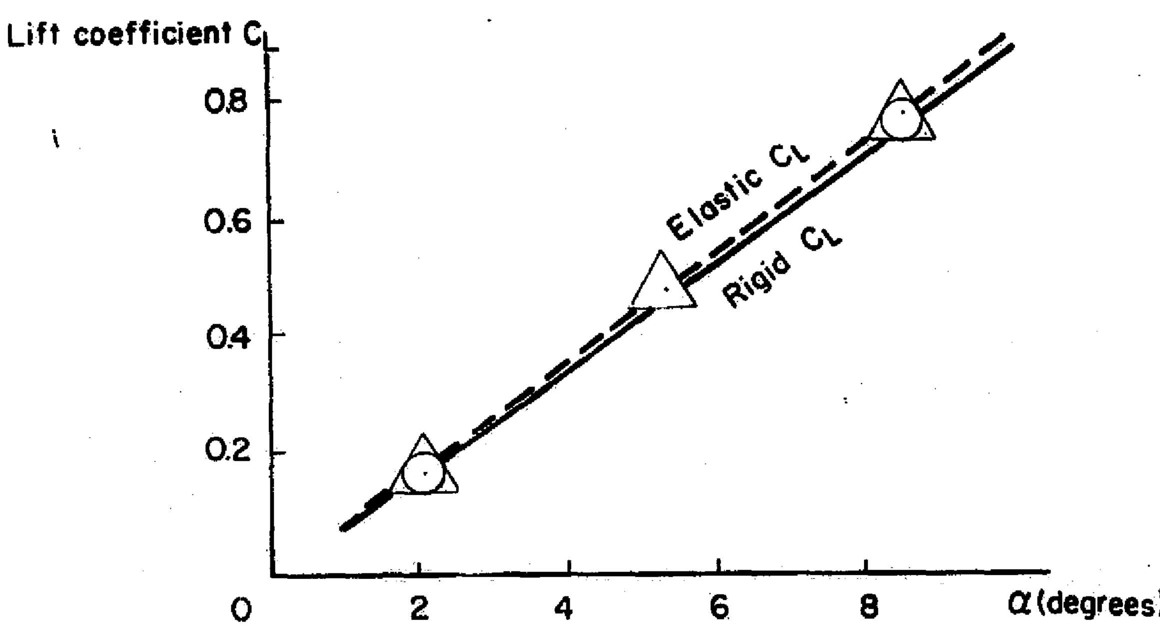

FIGURE II-b. Lift coefficient C_L versus angle of attack α, q=80 (leading edge).

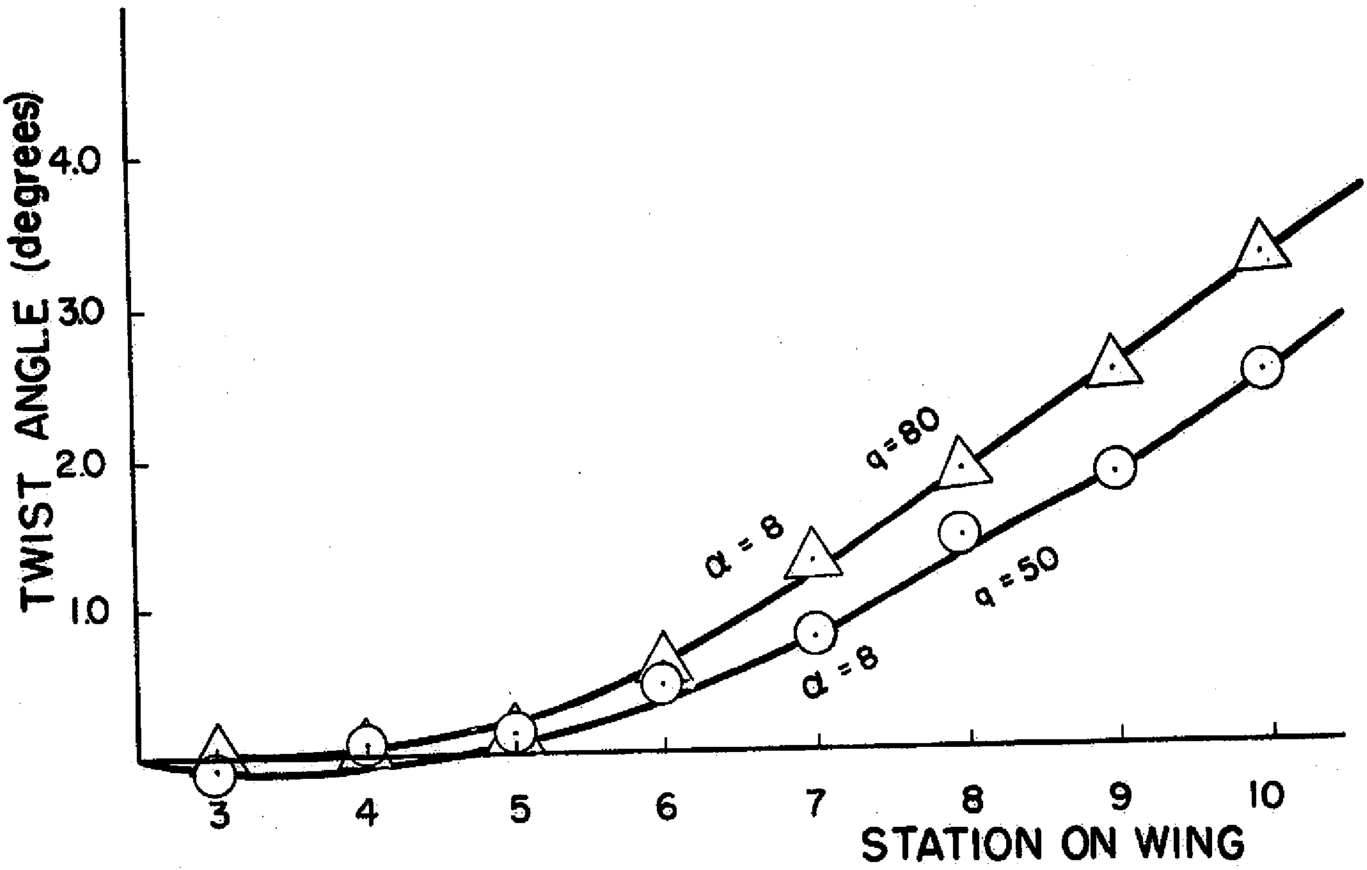

FIGURE 12. Plots of the twist angles measured from the wind tunnel.

angle of twist was measured at some of the inboard wing stations. Appendix B contains a tabulation of Wind Tunnel Test Results.

Finally, we wish to offer a comparison of experimental and theoretical aeroelastic estimates. The theoretical method outlined in Section III-C was used to estimate static aeroelasticity effects. The reader is reminded that the fuselage section of the orbiter was represented aerodynamically as a flat plate whose streamwise length corresponded to that of the wing root. Figure 13 shows a comparison of estimated and measurements for the wing leading edge z deflection. This Figure shows that this particular set of data correlated quite well. However, from Figure 14 we find that the theory estimates for elastic increment in angle of attack lie below those obtained experimentally. In an effort to determine if this difference was due to an inaccurate estimate of local center of pressure for each panel section, the centers of pressure were shifted forward by 20% and a new solution determined. While this does give better agreement, it does not appear that the solution to this discrepancy can be obtained by a simple center of pressure shift.

(VI) Discussion

In this report we have described the design, fabrication, testing, and analysis of a quasi-elastic orbiter model. The elasticity properties were introduced by constructing beam-like straight wings for the wind tunnel model. A standard influence coefficient mathematical model was used to estimate aeroelastic effects analytically. In general good agreement was obtained between the empirical and analytical estimates of the deformed shape. However in the static aeroelasticity case, we found that the physical wing exhibited less bending and more twist than was predicted by theory. Although the cause of this difference is yet unexplained, there are several factors that may have contributed to it:

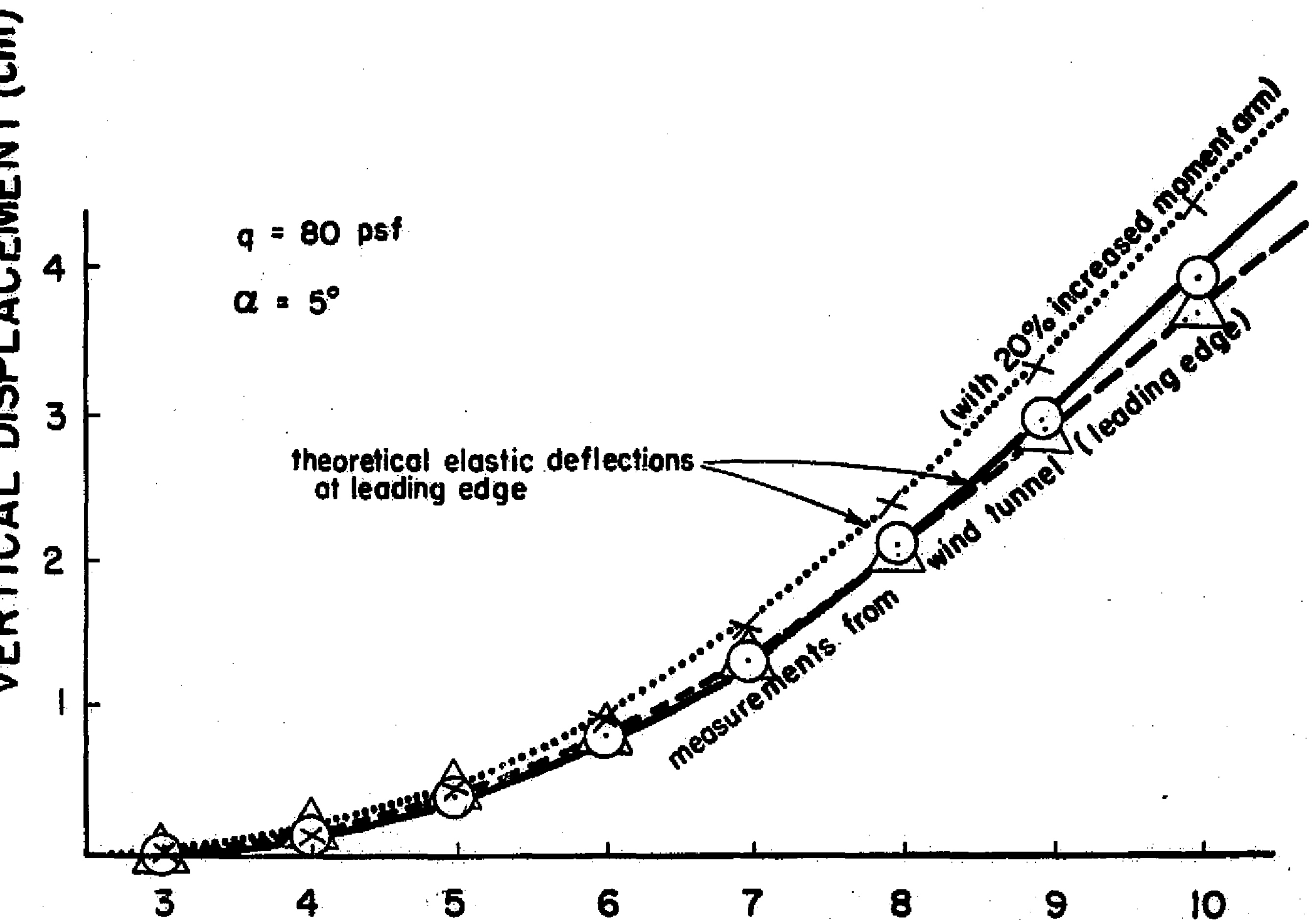

FIGURE 13. Comparison of the elastic deflections.

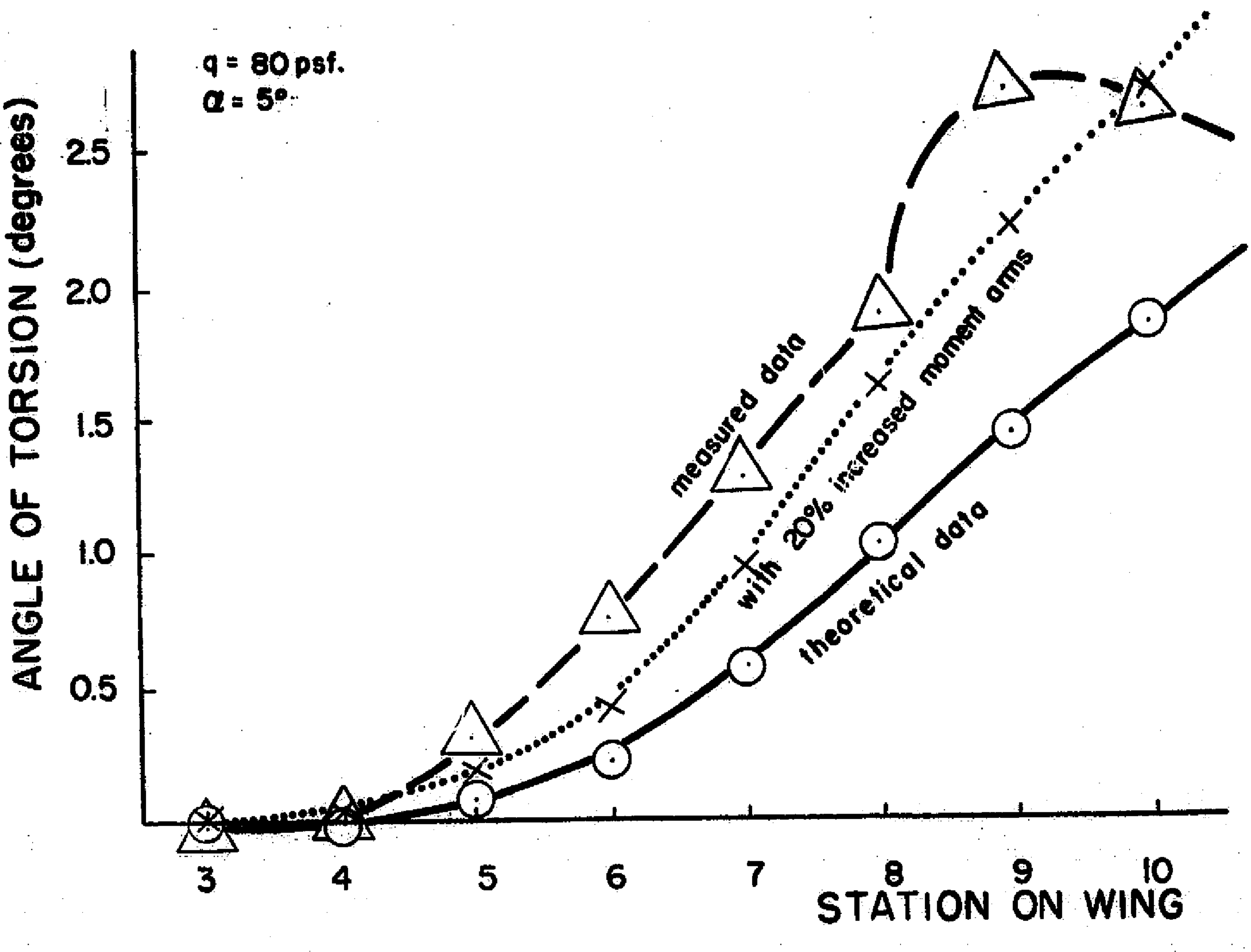

FIGURE 14. Comparison of twist angles.

1) Inadequate aerodynamic representation. (See above discussion)

2) Imprecise wind tunnel measurements. Although the wing was relatively quiet during testing some induced vibration occurred. This vibration along with cathatometer operator error almost certainly induced an unknown measurement error.

3) Structural Integrity. A continual problem that was experienced during testing was that the rib-spar weld joints could easily be destroyed by improper handling. This failure would explain spurious data points like the one at station 9 on Figure 14.

4) In-plane bending. The elastic wing was designed to have approximately the same stiffness in-plane as normal to the plane. Since the linear aerodynamic theory provides an inadequate representation for drag, it was not possible to adequately model this effect.

In summary, the results obtained in this report indicate that the linear aerodynamic and theories provide an approximate estimate of aeroelastic effects. However, our results imply that the theory underestimates (at least in this case) the elastic deformation in wing twist and hence the effects of elasticity on lift. We believe that further testing and more complete aerodynamic models are required to resolve this question.

References

[1] "A Method for Predicting the Stability Characteristic of an Elastic Airplane," Volume I, Theoretical Description by A. R. Dusto and others, D6-41064-1, December 1973.

[2] J. S. Przemieniecki, "Theory of Matrix Structural Analysis," McGraw-Hill Book Company, (1968).

[3] J. P. Giesing, T. P. Kalman, and W. P. Rodden, "Subsonic Unsteady Aerodynamics for General Configurations," Technical Report AFFDL-TR-71-5, Part I, Vol. I, (1971).

[4] I. S. Sokolnikoff, "Mathematical Theory of Elasticity," 2nd ed., New York, McGraw-Hill, 1956.

APPENDIX A

Aeroelasticity Computer Program Listing

The following pages contain a listing of the computer program used to compute the elastic displacements of the model wing.

```
//TB476    JOB (T907-,4-C--,*10,001,C-),'THISAYAKORN         '         ' JOB 958
//*WATFIV
C
C      ****************************************************************************
C      **                          DISPLACEMENT ON MODEL WING                    **
C      **                            CAUSED BY DYNAMIC LOAD                      **
C      ****************************************************************************
C
C          NOTATION
C
C      RLSPAR(J)=LENGTH OF J-TH SPAR (INCH)
C      M=NUMBER OF SPANWISE PANELS
C      NF=NUMBER OF DEGREES OF FREEDOM FOR EACH PANEL
C      EDP(J)      =JTH. ELEMENT OF THE ELASTIC DISPLACEMENT VECTOR
C      RDP(J)      =JTH. ELEMENT OF THE RIGID   DISPLACEMENT VECTOR
C
       IMPLICIT REAL*8 (A-H,O-Z)
       DIMENSION ESTIFF(6,6),ESTIF1(6,6),STIFF(24,24),DIFF(24,24)
       DIMENSION VEC1(24),VEC2(24)
       DIMENSION EI(8),GJ(8),EDP(24),RDP(24)
       COMMON /AREA1/ RLSPAR(8)
       COMMON /AREA2/          THETA1
       COMMON /AREA3/ DINV(60,60),RIBUH(10),RIBLH(10)
       COMMON /AREA4/ REDINV(48,60),A(24,30)
C
    40 FORMAT (10F12.3)
    42 FORMAT (4X, 8F15.5)
    44 FORMAT (3F15.6)
    46 FORMAT (T20,I2)
    48 FORMAT (8F15.6)
    50 FORMAT (8F10.6)
    52 FORMAT (8F10.3)
    54 FORMAT (8F15.5)
    70 FORMAT ('1')
    72 FORMAT ('-')
    74 FORMAT ('-',4X,'VALUES OF GJ (POUND-INCH SQUARED)')
    76 FORMAT ('-',4X,'VALUES OF EI (POUND-INCH SQUARED)')
    78 FORMAT ('-',4X,'LENGTH OF EACH SPAR (INCH)')
    80 FORMAT ('-',4X,'ELASTIC DISPLACEMENT VECTOR (ALONG THE MAJOR AXIS)
      1        ')
    82 FORMAT ('-',4X,'HERE IS THE STIFF-MATRIX')
    84 FORMAT ('-',T20,'REDUCED SIZE OF D-INVERSE MATRIX')
    86 FORMAT ('-',T20,'A-MATRIX')
    88 FORMAT ('-',T20,'MATRIX K- MATRIX A')
    91 FORMAT (7X,'INCH',T23,'RADIAN',T37,'RADIAN')
    94 FORMAT (4X,'ELASTIC DISPLACEMENT VECTOR (ALONG THE LEADING EDGE)')
    95 FORMAT (7X,'CENTIMETERS',T22,'DEGREES',T37,'DEGREES')
    96 FORMAT (4X,'ELASTIC DISPLACEMENT (ALONG THE TRAILING EDGE)')
C
       M=8
       MP2=M+2
       NF=6
       M3=(NF/2)*M
       THETA1=0.16872
C
       CALL DLM (BETA,SO,ALPHA,N)
C
C      REDUCE INVERSE D-MATRIX TO THE WORKABLE SIZE
       MN=M*N
       MNT=(M+2)*N
```

```
      IJ=0
      I2=0
      DO 890 J=1,N
      I2=I2+2
      DO 890 I=1,M
      IJ=IJ+1
      I2=I2+1
      KL=0
      DO 888 L=1,N
      DO 888 K=1,MP2
      KL=KL+1
      REDINV(IJ,KL)=DINV(I2,KL)
  888 CONTINUE
  890 CONTINUE
      PRINT 84
      DO 897 I=1,MN
      PRINT 46, I
      PRINT 42, (REDINV(I,J),J=1,MNT)
  897 CONTINUE
C
      CALL AMAT (M,N,M3,ALPHA,SO,  BETA,MSTAR)
C
C     PRINTOUT THE A-MATRIX
      PRINT 86
      DO 900 I=1,M3
      PRINT 46, I
      PRINT 40, (A(I,J),J=1,MSTAR)
  900 CONTINUE
C
C     READ IN INPUT-DATA
      READ 52, (GJ(J),J=1,M)
      READ 52, (EI(J),J=1,M)
      READ 50, (RLSPAR(J),J=1,M)
      DO 7 I=1,M
      GJ(I)=GJ(I)*1.120
    7 CONTINUE
C
C     PRINT OUT INPUT-DATA
      PRINT 70
      PRINT 74
      PRINT 54, (GJ(J),J=1,M)
      PRINT 76
      PRINT 54, (EI(J),J=1,M)
      PRINT 78
      PRINT 48, (RLSPAR(J),J=1,M)
C
      DO 14 I=1,M3
      DO 14 J=1,M3
   14 STIFF(I,J)=0.
      MM1=M-1
C
C     FORM GLOBAL STIFFNESS AND MASS MATRICES
      DO 32 I1=1,MM1
      I3M3=I1*3-3
      IF(I1.GT.1)GO TO 919
C
      CALL STIFFE (ESTIF1,GJ(1),EI(1),1,NF)
      CALL TRFORM (ESTIF1,THETA 1,NF)
      CALL STIFFE (ESTIFF,GJ(2),EI(2),2,NF)
      CALL TRFORM (ESTIFF,THETA 1,NF)
```

```
      C
            NFD2=NF/2
            DO 646 I=1,NFD2
            DO 646 J=1,NFD2
            ESTIFF (I,J)=ESTIFF(I,J)+ESTIF1(I+NFD2,J+NFD2)
        646 CONTINUE
            GO TO 929
        919 CONTINUE
            I1P1=I1+1
      C
            CALL STIFFE (ESTIFF,GJ(I1P1),EI(I1P1),I1P1,NF)
            CALL TRFORM (ESTIFF,THETA 1,NF)
      C
        929 CONTINUE
      C
      C     COMBINE ELEMENTAL MATRICES INTO GLOBAL MATRIX
            DO 13 J1=1,NF
            DO 13 K1=1,NF
            STIFF(I3M3+J1,I3M3+K1)=STIFF(I3M3+J1,I3M3+K1)+ESTIFF(J1,K1)
         13 CONTINUE
         32 CONTINUE
      C
      C     PRINT OUT THE STIFF-MATRIX
            PRINT 82
            DO 280 I=1,M3
            PRINT 46, I
            PRINT 54, (STIFF(I,J),J=1,M3)
        280 CONTINUE
      C
      C     MATRIX K- MATRIX A
      C
            DO 310 I=1,M3
            DO 310 J=1,M3
            DIFF(I,J)=STIFF(I,J)-A(I,J)
        310 CONTINUE
            GOTO 320
            PRINT 88
**WARNING**  UNNUMBERED EXECUTABLE STATEMENT FOLLOWS A TRANSFER
            DO 311 I=1,M3
            PRINT 46, I
            PRINT 54, (DIFF(I,J),J=1,M3)
        311 CONTINUE
        320 CONTINUE
      C
            CALL INVET (DIFF,M3,1.006)
      C
      C     GENERALIZED DISPLACEMENTS
            DO 332 I=1,M3
            VEC2(I)=0.0
            DO 332 J=1,MSTAR
            VEC2(I)=VEC2(I)+A(I,J)*ALPHA
        332 CONTINUE
            DO 360 I=1,M3
            EDP(I)=0.0
            DO 360 J=1,M3
            EDP(I)=EDP(I)+DIFF(I,J)*VEC2(J)
        360 CONTINUE
      C
      C     PRINT OUT DISPLACEMENT VECTOR
            PRINT 72
```

```
      PRINT 80
      PRINT 91
      PRINT 44, (EDP(L),L=1,M3)
      PRINT 72
      PRINT 94
      PRINT 95
      DO 400 I=1,M
      J=(I-1)*3+1
      K=(I-1)*3+2
      L=(I-1)*3+3
      PRINT 44, EDP(J)*2.540    +RIBUH(I  )*EDP(L)*2.540    ,EDP(K)*57.2
     1        95780,EDP(L)*57.295780
*EXTENSION*  OTHER COMPILERS MAY NOT ALLOW EXPRESSIONS IN OUTPUT LISTS
*EXTENSION*  OTHER COMPILERS MAY NOT ALLOW EXPRESSIONS IN OUTPUT LISTS
*EXTENSION*  OTHER COMPILERS MAY NOT ALLOW EXPRESSIONS IN OUTPUT LISTS
  400 CONTINUE
      PRINT 72
      PRINT 96
      PRINT 95
      DO 420 I=1,M
      J=(I-1)*3+1
      K=(I-1)*3+2
      L=(I-1)*3+3
      PRINT 44, EDP(J)*2.540    -RIBLH(I  )*EDP(L)*2.540    ,EDP(K)*57.2
     1        95780,EDP(L)*57.295780
*EXTENSION*  OTHER COMPILERS MAY NOT ALLOW EXPRESSIONS IN OUTPUT LISTS
*EXTENSION*  OTHER COMPILERS MAY NOT ALLOW EXPRESSIONS IN OUTPUT LISTS
*EXTENSION*  OTHER COMPILERS MAY NOT ALLOW EXPRESSIONS IN OUTPUT LISTS
  420 CONTINUE
C
   99 STOP
      END
C     ****************************************************************

      SUBROUTINE DLM (BETA,SO,ALPHA,N)
C
C     THE DOUBLET LATTICE PROCEDURE
C     FOR   STEADY-PLANAR,SUBSONIC,  COMPRESSIBLE FLOW.
C
C     INCREMENTAL OSCILLATORY DOWNWASH FACTORS
C     (BY FITTING THE KERNEL FUNCTION FOR LIFTING FUNCTIONS WITH A PARABOLA)
C
C     SYMBOLS:
C            ALPHA   =STATIC ANGLE OF ATTACK
C            ROOTLE=LOCATION OF THE ROOT POINT ON LEADING EDGE
C            ROOTTE=LOCATION OF THE ROOT POINT ON TRAILING EDGE
C            TIPLE =LOCATION OF THE TIP POINT ON LEADING EDGE
C            TIPTE =LOCATION OF THE TIP POINT ON TRAILING EDGE
C            M     =NUMBER OF COLUMNS OF WING PANELS (ON ONE WING)
C            N     =NUMBER OF PANELS PER COLUMN
C            (THE COLUMNS RUN FROM THE LEADING TO TRAILING EDGE OF THE WING)
C            B     =LENGTH OF SEMI-WING SPAN
C            PERCC(I)=PERCENTAGE OF CHORDWISE LOCATION ON THE WING
C            PERCS(J)=PERCENTAGE OF SPAN-WISE LOCATION ON THE WING
C            MU(I,J)=LENGTH OF EACH DOUBLET LINE
C            DELA(I,J)=AREA OF EACH WING PANEL
C            XI(I,J) =LOCATION OF EACH SENDING POINT ONT EACH PANEL
C            X (I,J) =LOCATION OF RECEIVING POINT ON EACH PANEL
C            AXSLP  =SLOPE OF MAJOR AXIS OF THE WING
C            XIAX(J)=XI COORDINATES OF EACH COLLUMN ALONG THE MAJOR AXIS
```

```
C             DELCP(I)=PRESSURE COEFFICIENTS ON ONE WING
C             VA        =SPEED OF SOUND
C             FMACH     =FREE STREAM MACH NUMBER
C             UINF      =FREE STREAM       VELOCITY
C
      IMPLICIT REAL*8 (A-H,O-Z)
      DIMENSION                    PCVSLP(6),SLOPE(6),PERCS(11),PERCC(7)
      DIMENSION XIIR(6),XIOR(6),XIID(6),XIOD(6),TANLAM(7)
      DIMENSION XII(7),XIO(7),Y(10),ETAC(10),XIAX(10),C(11),ETA(11)
      DIMENSION XI(6,10),XIC(6,10),X(6,10)
      DIMENSION                DELP(6,10),DELX(6,10),           R(6,10)
      DIMENSION DELC(6,11)
      REAL*8 LAMDA(6),LAMDAD(6),MU(6,10),ILEFT,IRIGHT
      COMMON /AREA3/ DRSS(60,60),RIBUH(10),RIBLH(10)
      COMMON /AREA5/ DELA(6,10),FL (6,10)
C
  200 READ (5,210,END=990) ROOTLE,ROOTTE,TIPLE,TIPTE,B,N,M,ALPHA
  210 FORMAT (5F10.3,2I10,F10.6)
      PRINT 220
  220 FORMAT ('1')
      PRINT 230
  230 FORMAT (4X,'DATA INPUT:- ')
      PRINT 240, ROOTLE,ROOTTE,TIPLE,TIPTE,B,M,N
  240 FORMAT (4X,'ROOTLE= ',F10.4,4X,'ROOTTE= ',F10.4,4X,'TIPLE= ',F10.4
     1       ,4X,'TIPTE= ',F10.4,4X,'B= ',F10.4,4X,'M= ',I4,4X,'N= ',I4)
      PRINT 250, ALPHA
  250 FORMAT ('-',4X,'ANGLE OF ATTACK IS ',F10.6)
C
      VA=1090.0
      W=0.0
      WK=0.0
      UINF=250.0
      FMACH=UINF/VA
      BETA=DSQRT(1.0-FMACH**2)
      B=B*BETA
      SQ=0.50*0.002503867*UINF**2
C
      PRINT 252, FMACH,BETA,SQ
  252 FORMAT (T20,'MACH NUMBER=',F10.6,T60,'BETA=',F10.6,T90,'DYNAMIC PR
     1ESSURE, Q=',F10.3)
C
C     PRECALCULATION FOR THE COORDINATES OF THE SENDING AND RECEIVING ELEMENTS
C     CALCULATION OF THE AREA OF EACH WING PANEL
      IN=N+1
      IM=M+1
      MN=M*N
      READ 254, (PERCS(J),J=1,IM)
      READ 254, (PERCC(I),I=1,IN)
  254 FORMAT (8F10.6)
      PRINT 258
  258 FORMAT ('-',4X,'PERCENT OF SPANWISE PANELING LOCATION')
      PRINT 305, (PERCS(J),J=1,IM)
      PRINT 260
  260 FORMAT ('-',4X,'PERCENT OF CHORDWISE PANELING LOCATION')
      PRINT 305, (PERCC(I),I=1,IN)
      DO 270 J=1,IM
      ETA(J)=B*PERCS(J)
  270 CONTINUE
      DO 280 I=1,IN
      XII(I)=(ROOTTE-ROOTLE)*PERCC(I)+ROOTLE
```

```
      XIO(I)=(TIPTE-TIPLE)*PERCC(I)+TIPLE
      TANLAM(I)=(XIO(I)-XII(I))/B
  280 CONTINUE
      C(1)=ROOTTE-ROOTLE
      C(IM)=TIPTE-TIPLE
      AXSLP=(TIPLE-ROOTLE+0.3750*(C(IM)-C(1)))/B
      AXDEG=57.295780*DATAN(AXSLP)
      PRINT 284, AXDEG
  284 FORMAT ('-','SLOPE OF MAJOR AXIS =',F16.6,' DEGREES')
C
C     SLOPE OF LINE DOUBLETS, SLOPE, WITH ITS ANGLE, LAMDA.
      DO 370 I=1 ,N
      DO 300 J=1,IM
      C(J)=C(1)-(C(1)-C(IM))*PERCS(J)
      DELC(I,J)=(PERCC(I+1)-PERCC(I))*C(J)
  300 CONTINUE
      XIID(I)=XII(I)+0.250  *DELC(I,1)
      XIOD(I)=XIO(I)+0.250*DELC(I,IM)
      SLOPE(I)=(XIOD(I)-XIID(I))/B
      LAMDA(I)=DATAN(SLOPE(I))
      LAMDAD(I)=LAMDA(I)*57.295780
      XIIR(I)=XII (I)+0.750  *DELC(I,1)
      XIOR(I)=XIO(I)+0.750  *DELC(I,IM)
  370 RCVSLP(I)=(XIOR(I)-XIIR(I))/B
      PRINT 380
  380 FORMAT ('-',4X,'ANGLE OF EACH DOUBLET LINE (IN DEGREES)')
      PRINT 305, (LAMDAD(I),I=1,N)
  305 FORMAT (4X,F16.6)
C
C
C     NOW COMPUTING THE REQUIRED COORDINATES
      IJ=0
      DO 405 I=1,N
      DO 405 J=1,M
      MU(I,J)=(ETA(J+1)-ETA(J))/DCOS(LAMDA(I))
      INDEXJ=2*(M-J)+1
      DELA(I,J)=0.50D0*DELC(I,J)*(ETA(J+1)-ETA(J))*(C(1)*INDEXJ
     1       +C(IM)*(2*J-1))/(C(1)*M)
      DELA(I,J)=DELA(I,J)/BETA
      IJ=IJ+1
      XI(I,J)=XIID(I)+ETA(J   )*SLOPE(I)
      ETAC(J)=0.50*(ETA(J)+ETA(J+1))
      Y(J)=ETAC(J)
      X(I,J)=XIIR(I)+RCVSLP(I)*Y(J)
      DELX(I,J)=0.50*(DELC(I,J)+DELC(I,J+1))
      XIC(I,J)=X(I,J)-0.50*DELX(I,J)
      XIAX(J)=0.3750*C(1)+AXSLP*Y(J)+ROOTLE
      FL(I,J)=XIC(I,J)-XIAX(J)
      R(I,J)=X(I,J)-XIAX(J)
      RIBUH(J)=(C(J)+C(J+1))/2.0*0.3750
      FIBLH(J)=RIBUH(J)*0.6250/0.3750
  405 CONTINUE
      PRINT 308
  308 FORMAT ('-','XI-LOCATIONS ALONG THE MAJOR AXIS:-')
      PRINT 340, (XIAX(K),K=1,M)
      PRINT 310
  310 FORMAT ('-',4X,'HERE IS THE VECTOR OF MU
      DO 311 I=1,N
      PRINT 330
      PRINT 340, (MU(I,J),J=1,M)
```

```
  311 CONTINUE
C     PRINT 314
C 314 FORMAT ('-',4X,'X-LOCATIONS OF EACH RECEIVING POINT')
C     PRINT 330
C     PRINT 340, ((X(I,J),J=1,M),I=1,N)
      PRINT 320
  320 FORMAT ('-',4X,'PANEL AREA ON ONE WING')
      DO 350 I=1,N
      PRINT 330
  330 FORMAT ('-')
      PRINT 340, (DELA(I,J),J=1,M)
  340 FORMAT (4X,10F12.6)
  350 CONTINUE
      PRINT 352
  352 FORMAT ('-',T20,'L(I,J) WITH SIGN OF THEIR X-COORDINATE LOCATION B
     1EING CARRIED ALONG')
      DO 353 I=1,N
      PRINT 330
      PRINT 340, (FL(I,J),J=1,M)
  353 CONTINUE
      PRINT 354
  354 FORMAT ('-',T20,'R(I,J) WITH SIGN OF THEIR X-COORDINATE LOCATION B
     1EING CARRIED ALONG')
      DO 355 I=1,N
      PRINT 330
      PRINT 340, (R(I,J),J=1,M)
  355 CONTINUE
C
C     NOW CALCULATE DRS(1) AND DRS(S) MATRICES
C     PRINT 360
C 360 FORMAT ('-',18X,'DRSS',20X,'DRSI')
      T1=1.0
      KL=0
      DO 590 K=1,N
      DO 590 L=1,M
      KL=KL+1
      IJ=0
C     PRINT 415
C 415 FORMAT ('-')
C     PRINT 363, KL
      DO 580 I=1,N
C     PRINT 315
C 315 FORMAT (4X,'     ')
      DO 580 J=1,M
      IJ=IJ+1
      XMXI=X(K,L)-XI(I,J)
      YMETA=    Y(L)-ETA(J)
      YPETA=Y(L)+ETA(J)
      XMXIC=X(K,L)-XIC(I,J)
      YMETAC=    Y(L)-ETAC(J)
      YPETAC=Y(L)+ETAC(J)
      ROOT= DSQRT(MU(I,J)**2-2.0  *(XMXI*DSIN(LAMDA(I))
     1      +YMETA*DCOS(LAMDA(I)))*MU(I,J)+XMXI**2+YMETA**2)
      IRIGHT=MU(I,J)/(YMETA*(Y(L)-ETA(J+1)))+(ROOT/(Y(L)-ETA(J+1))
     1      - DSQRT(XMXI**2+YMETA**2)/YMETA)/(XMXI*DCOS(LAMDA(I))
     2      -YMETA*DSIN(LAMDA(I)))
      ROOT= DSQRT(MU(I,J)**2-2.0  *(XMXI*DSIN(LAMDA(I))
     1      -YPETA*DCOS(LAMDA(I)))*MU(I,J)+XMXI**2+YPETA**2)
      ILEFT=MU(I,J)/(YPETA*(Y(L)+ETA(J+1)))-(ROOT/(Y(L)+ETA(J+1))
     1      - DSQRT(XMXI**2+YPETA**2)/YPETA)/(XMXI*DCOS(LAMDA(I)))
```

```
     2         +YPETA*DSIN(LAMDA(I)))
C         DRSS=(IRIGHT+ILEFT)*DCOS(LAMDA(I))
C         IF (W.EQ.0.0) GOTO 492
          DRSS(KL,IJ)=(IRIGHT+ILEFT)*DCOS(LAMDA(I))
          DRSS(KL,IJ)=DRSS(KL,IJ)*0.50*DELX(I,J)/4.0/3.14159265360
C
C         TRANSFORM BACK TO THE ORIGINAL Y-AXIS
          YMETA=YMETA/BETA
          YPETA=YPETA/BETA
          YMETAC=YMETAC/BETA
          YPETAC=YPETAC/BETA
  580 CONTINUE
  590 CONTINUE
C
          CALL INVPT (DRSS,MN,1.0D0)
C
          DO 600 I=1,N
          DO 600 J=1,M
          FL (I,J)=FL (I,J)/BETA
  600 CONTINUE
          GOTO 200
  990 CONTINUE
          RETURN
          END
C     **********************************************************************

          SUBROUTINE STIFFE (ESTIFF,EGJ,EEI,N,NF)
          IMPLICIT REAL*8 (A-H,O-Z)
          DIMENSION ESTIFF(NF,NF)
          COMMON /AREA1/ RLSPAR(8)
C
          RLC =RLSPAR(N)
          RLC2=RLC**2
          RLC3=RLC**3
C
C         FORM BENDING STIFFNESS MATRIX-
          DO 40 I=1,NF
          DO 40 J=1,NF
          ESTIFF(I,J)=0.0
   40 CONTINUE
          ESTIFF(1,1)=12./RLC3*EEI
          ESTIFF(1,2)=6./RLC2*EEI
          ESTIFF(1,4)=-12./RLC3*EEI
          ESTIFF(1,5)=6./RLC2*EEI
          ESTIFF(2,1)=ESTIFF(1,2)
          ESTIFF(2,2)=4./RLC*EEI
          ESTIFF(2,4)=-6./RLC2*EEI
          ESTIFF(2,5)=2./RLC*EEI
          ESTIFF(4,1)=ESTIFF(1,4)
          ESTIFF(4,2)=ESTIFF(2,4)
          ESTIFF(4,4)=ESTIFF(1,1)
          ESTIFF(4,5)=-6./RLC2*EEI
          ESTIFF(5,1)=ESTIFF(1,5)
          ESTIFF(5,2)=ESTIFF(2,5)
          ESTIFF(5,4)=ESTIFF(4,5)
          ESTIFF(5,5)=ESTIFF(2,2)
C
C         FORM TORSIONAL STIFFNESS MATRIX-
          ESTIFF(3,3)=EGJ/RLC
          ESTIFF(6,3)=-EGJ/RLC
```

```
      ESTIFF(3,6)=ESTIFF(6,3)
      ESTIFF(6,6)=ESTIFF(3,3)
      RETURN
      END
C     **********************************************************************

      SUBROUTINE TRFORM (A,THETAT,NF)
      IMPLICIT REAL*8 (A-H,O-Z)
      DIMENSION A(NF,NF),TRANS(6 ,6 ),PROD(6 ,6 )
C
      DO 44 I=1,NF
      DO 44 J=1,NF
   44 TRANS(I,J)=0.0
      TRANS(1,1)=1.0
      TRANS(4,4)=1.0
      TRANS(2,2)=DCOS(THETAT)
      TRANS(2,3)=-DSIN(THETAT)
      TRANS(3,2)=DSIN(THETAT)
      TRANS(3,3)=DCOS(THETAT)
      TRANS(5,5)=DCOS(THETAT)
      TRANS(5,6)=-DSIN(THETAT)
      TRANS(6,5)= DSIN(THETAT)
      TRANS(6,6)=DCOS(THETAT)
      DO 51 I=1,NF
      DO 51 J=1,NF
      PROD(I,J)=0.
      DO 52 K=1,NF
   52 PROD(I,J)=PROD(I,J)+TRANS(K,I)*A(K,J)
   51 CONTINUE
      DO 53 I=1,NF
      DO 53 J=1,NF
      A(I,J)=0.0
      DO 54 K=1,NF
   54 A     (I,J)=A     (I,J)+PROD(I,K)*TRANS(K,J)
   53 CONTINUE
      RETURN
      END
C     **********************************************************************

      SUBROUTINE AMAT (M,N,M3,ALPHA,SO,  BETA,MSTAR)
C
C     SYMBOLS:-
C     THETA1        =ANGLE FROM ELASTIC AXIS ONTO THE Y-AXIS
C     THETA2        =ANGLE FROM  LINE OF LOADINGS ONTO THE Y-AXIS
C     B             =SEMI-SPANWISE LENGTH
C     ROOTLE        =LOCATION OF THE ROOT POINT ON LEADING EDGE
C     ROOTTE        =LOCATION OF THE ROOT POINT ON TRAILING EDGE
C     TIPLE         =LOCATION OF THE TIP POINT ON LEADING EDGE
C     TIPTE         =LOCATION OF THE TIP POINT ON TRAILING EDGE
C     AATDEG        =ANGLE OF ATTACK IN DEGREES
C     EXF(L1)       =VERTICAL FORCE LOAD ONTO THE J-TH. SECTION OF THE WING
C     EXF(L2)       =BENDING MOMENT LOAD ONTO THE WING (EQUALS ZERO IN HERE)
C     EXF(L3)       =TORSIONAL MOMENT LOAD ONTO THE J-TH. SECTION OF THE WING
C                    (CAUSED BY VERTICAL FORCE APPLIED OFF FROM THE MAJOR AXIS)
C     Y(J)          =Y-LOCATION OF EACH WING SECTION
C     XAX(J)        =X-LOCATION ALONG THE MAJOR AXIS
C     XLD(J)        =X-LOCATION ALONG THE LINE OF LOADING ON THE WING
C     ARM(J)        =TORSIONAL MOMENT ARM OF THE J-TH. SECTION
C     BLC           =SPANWISE LENGTH OF EACH PANEL
C     FF(I,J)       =CONDENSED CIRCULATION MATRIX
```

```
C       DPC(J)        =DISTANCE OF DYNAMIC PRESSURE OFF FROM THE MAJOR AXIS
C
        IMPLICIT REAL*8 (A-H,O-Z)
C       DIMENSION ETA(MP1)
        DIMENSION ETA(9),DPC(8),FLD(48)
        DIMENSION ARM(8),F(8,10),     XAX(8),XLD(8),Y(8)
        DIMENSION            CLA( 8,10),DEL CP(48,10)
        COMMON /AREA2/         THETA1
        COMMON /AREA4/ REDINV(48,60),A(24,30)
        COMMON /AREA5/ DELA(6,10),FL (6,10)
C
      2 FORMAT (8F10.6)
      8 FORMAT ('-',4X,'ACTUAL MOMENT ARM OF EACH COLUMN (ALONG THE SPAN)'
     1       )
C
        THETA2=0.20362
        ROOTLE=0.0
        ROOTTE=10.0050
        TIPTE=10.0050
        TIPLE=5.980
        B=21.80
C
C       CALCULATE DISTANCE OFF FROM THE MAJOR AXIS OF EACH STATION
        MP1=M+1
        MP2=M+2
        MSTAR=M3+6
        DO 30 J=1,MP1
        ETA(J)=B*(J-1)/M
     30 CONTINUE
        DO 40 J=1,M
        Y(J)=0.50*(ETA(J)+ETA(J+1))
        X AX(J)=ROOTLE+0.3750*(ROOTTE-ROOTLE)+Y(J)*DTAN(THETA1)
        X LD(J)=ROOTLE+0.250 *(ROOTTE-ROOTLE)+Y(J)*DTAN(THETA2)
        ARM(J)=X AX(J)-X LD(J)
     40 CONTINUE
        MN=M*N
        DO 43 I=1,MN
        DO 43 J=1,MP2
        DEL CP(I,J)=0.0
        DO 42 K=1,N
        L=(K-1)*MP2
        DEL CP(I,J)=DEL CP(I,J)-REDINV(I,J+L)
     42 CONTINUE
     43 CONTINUE
        DO 45 I=1,M
        DO 45 J=1,MP2
        CLA(I,J)=0.0
        DO 44 K=1,N
        L=(K-1)*M
        CLA(I,J)=CLA(I,J)+DEL CP(I+L,J)/BETA*DELA(K,I+2)
     44 CONTINUE
        F (I,J)=CLA(I,J)*S0/144.0
     45 CONTINUE
C
C       FIND THE EXACT LOCATION OF DYNAMIC PRESSURE
        MNES=MP2*N
        DO 60 I=1,MN
        FLD(I)=0.0
        DO 60 J=1,MNES
        FLD(I)=FLD(I)-REDINV(I,J)
```

ORIGINAL PAGE IS
OF POOR QUALITY

```
   60 CONTINUE
      DO 65 J=1,M
      REP1=0.0
      REP2=0.0
      DO 62 I=1,N
      K=(I-1)*M+J
      FLD(K)=FLD(K)*DELA(I,J+2)/BETA
      FLD(K)=FLD(K)*SQ/144.0
      REP1=REP1+FLD(K)
      REP2=REP2-FL(I,J+2)*FLD(K)
   62 CONTINUE
      DPC(J)=REP2/REP1
      DPC(J)=DPC(J)*1.20
   65 CONTINUE
C
C     PRINT OUT THE MOMENT ARM
      PRINT 8
      PRINT 2, (DPC(J),J=1,M)
C
C     COMPARE TO THE QUATER CHORD MOMENT ARM
      PRINT 2, (ARM(J),J=1,M)
C
C     FORM  COEFFICIENT  MATRIX FOR EXTERNAL LOAD
      DO 50 I=1,M3
      DO 50 J=1,MSTAR
      A(I,J)=0.0
   50 CONTINUE
      DO 55 I=1,M
      ARM(I)=DPC(I)
      I3=I*3
      DO 55 J=1,MP2
      J3=J*3
      A(I3-2,J3)=F(I,J)
      A(I3,J3)=F(I,J)*ARM(I)*DCOS(ALPHA)
   55 CONTINUE
      RETURN
      END
C     ************************************************************************

      SUBROUTINE INVRT(A,N,SCALE)
      IMPLICIT REAL*8 (A-H,O-Z)
      DIMENSION A(N,N),INDEX(90,2),IPVOT(90),PIVOT(90)
C     CALL ERRSET(207,256,0,1)
C
C     SCALE  DOWN MATRIX A
      DO 1 I=1,N
      DO 1 J=1,N
    1 A(I,J)=A(I,J)/SCALE
      ONE=1.0
      ZERO=0.0
   57 DET=ONE
      DO 17 J=1,N
   17 IPVOT(J)=0
      DO 135 I=1,N
C     FOLLOWING 12 STATEMENTS FOR SEARCH FOR PIVOT ELEMENT
      T=ZERO
      DO 9 J=1,N
      IF(IPVOT(J)-1) 13,9,13
   13 DO 23 K=1,N
      IF(IPVOT(K)-1) 43,23,81
```

```
   43 IF(DABS(T)-DABS(A(J,K))) 83,23,23
   83 IROW=J
      ICOL=K
      T=A(J,K)
   23 CONTINUE
    9 CONTINUE
      IPVOT(ICOL)=IPVOT(ICOL)+1
C     FOLLOWING 15 STATEMENTS PUT PIVOL ELEMENT ON DIAGONAL
      IF(IROW-ICOL) 73,109,73
   73 DET=-DET
      DO 12 L=1,N
      T=A(IROW,L)
      A(IROW,L)=A(ICOL,L)
   12 A(ICOL,L)=T
  109 INDEX(I,1)=IROW
      INDEX(I,2)=ICOL
      PIVOT(I)=A(ICOL,ICOL)
      DET=DET*PIVOT(I)
C     FOLLOWING 6 STATEMENTS TO DIVIDE POVOT ROW BY PIVOT ELEMENT
      A(ICOL,ICOL)=ONE
      DO 205 L=1,N
  205 A(ICOL,L)=A(ICOL,L)/PIVOT(I)
C     FOLLOWINT 10 STATEMENTS TO REDUCE NON-PIVOT ROWS
      DO 135 LI=1,N
      IF(LI-ICOL) 21,135,21
   21 T=A(LI,ICOL)
      A(LI,ICOL)=ZERO
      DO 89 L=1,N
   89 A(LI,L)=A(LI,L)-A(ICOL,L)*T
  135 CONTINUE
C     FOLLOWINT 11 STATEMENTS TO INTERCHANGE COLUMNS
  222 DO 3 I=1,N
      L=N-I+1
      IF(INDEX(L,1)-INDEX(L,2)) 19,3,19
   19 JROW=INDEX(L,1)
      JCOL=INDEX(L,2)
      DO 549 K=1,N
      T=A(K,JROW)
      A(K,JROW)=A(K,JCOL)
      A(K,JCOL)=T
  549 CONTINUE
    3 CONTINUE
   81 CONTINUE
C
C     SCALE BACK INVERSE OF MATRIX-A
      DO 2 I=1,N
      DO 2 J=1,N
    2 A(I,J)=A(I,J)/SCALE
      RETURN
C  31 RETURN
      END

//DATA
***ERROR***  INSUFFICIENT MEMORY TO ASSIGN ARRAY STORAGE. JOB ABANDONED

CORE USAGE      OBJECT CODE=   26312 BYTES,ARRAY AREA=   82752 BYTES,TOTAL AREA AVAILABLE=  104544  BYTES

DIAGNOSTICS         NUMBER OF ERRORS=       1, NUMBER OF WARNINGS=       1, NUMBER OF EXTENSIONS=       6

COMPILE TIME=     6.68 SEC,EXECUTION TIME=     0.00 SEC,   TAMU/WATFIV - VER 1 LEV 3 JANUARY 1972     DATE=  74/217
```

APPENDIX B

Tabulation of Wind Tunnel Data

S_{REF} = 423.06 sq. in., $\bar{C}$ = 8.36 in.

I) q_∞ = 50

LEADING EDGE	STATION NUMBER ON WING	VERTICAL DEFLECTION	
		δ_{LE}	δ_{TE}
α = 2.13	3	0.007	-0.015
C_L = 0.1683	4	0.036	-0.015
C_D = 0.1037	5	0.083	0.042
C_{PM} = -0.1684			
TRAILING EDGE	6	0.176	0.196
α = 2.13	7	0.301	0.239
C_L = 0.1679	8	0.45	0.301
C_D = 0.1016	9	0.584	0.486
C_{PM} = -0.1635	10	0.731	0.682

LEADING EDGE	STATION NUMBER ON WING	VERTICAL DEFLECTION	
		δ_{LE}	δ_{TE}
α = 5.37	3	-0.029	0.028
C_L = 0.461	4	0.064	0.079
C_D = 0.1215	5	0.21	0.163
C_{PM} = -0.3301			
TRAILING EDGE	6	0.442	0.379
α = 5.37	7	0.752	0.662
C_L = 0.4675	8	1.174	0.985
C_D = 0.1242	9	1.617	1.456
C_{PM} = -0.3341	10	2.096	2.005

LEADING EDGE	STATION NUMBER	VERTICAL DEFLECTION	
α = 8.61	ON WING	δ_{LE}	δ_{TE}
C_L = 0.758	3	0.021	0.058
C_D = 0.1495	4	0.19	0.163
C_{PM} = -0.4591	5	0.442	0.395
TRAILING EDGE	6	0.849	0.71
α = 8.6	7	1.406	1.182
C_L = 0.7521	8	2.089	1.724
C_D = 0.1505	9	2.905	2.491
C_{PM} = -0.4552	10	3.742	3.258

II) q_∞ = 80

LEADING EDGE	STATION NUMBER	VERTICAL DEFLECTION	
α = 2.13	ON WING	δ_{LE}	δ_{TE}
C_L = 0.1676	3	0.021	-0.22
C_D = 0.1059	4	0.064	0.035
C_{PM} = -0.1671	5	0.132	0.098
TRAILING EDGE	6	0.282	0.203
α = 2.13	7	0.463	0.324
C_L = 0.167	8	0.718	0.457
C_D = 0.1033	9	0.908	0.747
C_{PM} = -0.1665	10	1.175	1.019

LEADING EDGE	STATION NUMBER	VERTICAL DEFLECTION	
α = 5.38	ON WING	δ_{LE}	δ_{TE}
C_L = 0.4779	3	0	0.02
C_D = 0.1254	4	0.149	0.155
C_{PM} = -0.3443	5	0.408	0.296
TRAILING EDGE	6	0.78	0.535
α = 5.38	7	1.323	0.95
C_L = 0.4759	8	2.048	1.562
C_D = 0.1252	9	2.898	2.286
C_{PM} = -0.3437	10	3.678	3.165

LEADING EDGE	STATION NUMBER	VERTICAL DEFLECTION	
α = 8.62	ON WING	δ_{LE}	δ_{TE}
C_L = 0.7728	3	0.048	0.037
C_D = 0.1540	4	0.268	0.236
C_{PM} = -0.4776	5	0.639	0.591
TRAILING EDGE	6	1.335	1.153
α = 8.62	7	2.251	1.891
C_L = 0.7732	8	3.356	2.87
C_D = 0.1503	9	4.682	4.115
C_{PM} = -0.4784	10	6.136	5.505